

OPTIMAL MANAGEMENT OF SEASONAL PUMPED HYDRO STORAGE IN
UAE

by

Asmaa Ibrahim Abdelfattah

A Thesis presented to the faculty of the
American University of Sharjah
College of Engineering
In Partial Fulfilment
of the Requirements
for the Degree of

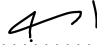
Master of Science in
Electrical Engineering

Sharjah, United Arab Emirates

November 2022

Declaration of Authorship

I declare that this thesis is my own work and, to the best of my knowledge and belief, it does not contain material published or written by a third party, except where permission has been obtained and/or appropriately cited through full and accurate referencing.

Signed... Asmaa Ibrahim Abdelfattah 

Date. Feb 22nd, 2023

The Author controls copyright for this report.

Material should not be reused without the consent of the author. Due acknowledgement should be made where appropriate.

© Year 2022

Asmaa Ibrahim Abdelfattah

ALL RIGHTS RESERVED

Approval Signatures

We, the undersigned, approve the Master's Thesis of Asmaa Ibrahim Abdelfattah

Thesis Title: Optimal Management of Seasonal Pumped Hydro Storage in UAE

Date of Defense: 28th November, 2022

Name, Title and Affiliation

Signature

Dr. Ahmed Othman
Professor, Department of Electrical Engineering
Thesis Advisor

Dr. Mostafa Shaaban
Associate Professor, Department of Electrical Engineering
Thesis Co-Advisor

Dr. Hasan Mir
Professor, Department of Electrical Engineering
Thesis Committee Member

Dr. Md. Maruf Mortula
Professor, Department of Civil Engineering
Thesis Committee Member

Dr. Mostafa Shaaban
Interim Head
Department of Electrical Engineering

Dr. Lotfi Romdhane
Associate Dean for Graduate Affairs and Research
College of Engineering

Dr. Fadi Aloul
Dean
College of Engineering

Dr. Mohamed El-Tarhuni
Vice Provost for Research and Graduate Studies
Office of Research and Graduate Studies

Acknowledgements

I want to express my deepest gratitude to Allah, for every time I thought I can not finish this work, he showed me that I could.

I want to express my most profound appreciation to my thesis Supervisors, Dr. Ahmed Othman and Dr. Mostafa Shaaban, for their support during this journey, discussions, time, and valuable suggestions.

I want also to thank my examination committee members, Dr. Hasan Mir and Dr. Md. Mortula. Their feedback was greatly appreciated.

Also, I thank Dr. Mohamed Abdelgawad from the department of mechanical Engineering for his help to answer my questions.

I also must express my utmost thanks to my friends for any help that pushed me through, no matter how small it was.

Lastly, I'd like to mention that I'm thankful to my parents for their continuous love and support.

Dedication

To my parents, sister, and nephew Omar, the Joy of my life...

Abstract

Power demand varies with the time of day and with seasons. Responding to changing demand over time, especially during peak times, is challenging for Energy suppliers. UAE annual demand curve is characterized to be high in seasonal variation. This causes peak power plants to operate more in the highest demand seasons, usually summer, increasing the cost of electricity and the operation of expensive power plants. Peak load shaving is making the load curve flatten by reducing the peak load and shifting it to times of lower demand and hence reduce the operation of expensive power plants.

Possible solutions for demand curve flattening are switching off equipment or load-shifting techniques through demand side management (DSM), also through electrical vehicles (EV) integration, and Energy Storage Systems (ESS). However, DSM and EV integration are not applicable solutions for seasonal variation as the peak is mainly driven by the Air conditioning loads. Hence, there is a need for large-scale and long-term ESS to store energy in the time of low-demand seasons for future utilization in the highest-demand ones.

This research aims to develop an Energy Management System (EMS) that optimally manages a grid-connected pumped hydro storage (PHS) unit to achieve the purpose of peak shaving. The proposed framework analyses the seasonal performance of PHS in supporting the grid in the UAE and reflects the possible economic benefits considering transmission constraints, optimal power flow, hydraulic model, and losses over a study period of one year. The proposed model incorporates dynamic economic dispatch (DED) over a relatively long period; hence DC power flow analysis is considered to ensure fast load flow estimation.

This analysis is essential to motivate the construction of new seasonal PHS plants due to the high construction cost they are identified with, especially in geographical areas where this technology is not yet considered and is hard to construct

Keywords: Pumped Hydro Storage, Optimal Management, Optimization, Renewable Energy Resources

Table of Contents

Abstract	6
List of Figures	9
List of Tables	10
List of Abbreviations	11
Chapter 1. Introduction	12
1.1. Introduction	12
1.2. Overview	12
1.3. Thesis objectives	16
1.4. Research contribution	16
1.5. Thesis organization	16
Chapter 2. Background and Literature Review	18
2.1. PHS fundamentals	18
2.1.1. PHS configuration	18
2.1.2. PHS power equation	19
2.1.3. Hydraulic head	19
2.1.4. Hydropower generator	21
2.2. DC power flow	22
2.3. Dynamic economic dispatch	23
2.4. Literature review	24
Chapter 3. Methodology	29
3.1. Network mathematical model	29
3.1.1. PHS unit model	29
3.1.2. DC power flow model	33
3.1.3. Dynamic economic dispatch	34
3.1.4. Problem formulation	35
3.2. Case study: data collection and preparation	38
3.2.1. Study period and demand data	38
3.2.2. 24bus-IEEE RTS bus system	39
3.2.3. PHS unit assumptions and parameters	41
3.3. Optimization tool	44

Chapter 4.	Results and Analysis	45
4.1.	Peak shaving affect	45
4.2.	Storage: charging and discharging	46
4.3.	Cost of operation	48
4.4.	Performance evaluation	49
Chapter 5.	Conclusion and Future Work	51
References		52
Appendix A		58
Vita		59

List of Figures

Figure 1-1:Peak Shaving[2]	13
Figure 1-2: UAE annual demand curve	14
Figure 1-3: Electrical storage technologies.....	15
Figure 2-1:Bernoulli Principle	22
Figure 2-2: illustration of the constant-speed (a) and variable speed operation [24] (b)	22
Figure 3-1:Proposed Methodology	29
Figure 3-2:Proposed system Diagram[52]	37
Figure 3-3 proposed IEEE24 bus system with PHS unit at bus 19.....	39
Figure 3-4: PHS unit Energy Capacity Parameters.....	42
Figure 4-1:Difference in thermal unit's energy production after PHS unit integration	46
Figure 4-2:Generation cost for the thermal units per MW	46
Figure 4-3: Average hourly demand for each season in UAE.....	47
Figure 4-4:Annual level of the UR with proposed charging and discharging capacity	47
Figure 4-5: Annual level of the UR with decreased charging and discharging capacity	48
Figure 4-6: Annual level of the UR with increased charging and discharging capacity	48

List of Tables

Table 1-1: Comparison of ESS[12].....	17
Table 3-1: Optimization Problem Variables	38
Table 3-2: IEEE RTS 24-bus system branch data	40
Table 3-3: Thermal Generating units' data	40
Table 3-4: Demand Details	41
Table 3-5: Assumptions for charging and discharging capacities	43
Table 3-6: Penstock Technical Parameters	43
Table 4-1: Thermal unit's energy production before and after PHS unit integration ...	45
Table 4-2: PHS parameters	47
Table 4-3: Operation cost with different PHS unit storage capacities	49
Table 4-4: Operation cost increasing charging and discharging capacities	49

List of Abbreviations

COP21	Conference of the Parties
DED	Dynamic Economic Dispatch
DSM	Demand Side Management
DFIG	Doubly Fed Induction Generator
ED	Economic Dispatch
EMS	Energy Management system
ESS	Energy Storage System
EMS	Energy Management System
EV	Electric Vehicle
NLP	Nonlinear Problem
NiCd	Nickel-cadmium
OPF	Optimal Power flow
PHS	Pumped Hydro Storage
RTS	Reliability Test System
SED	Static Economic Dispatch
NaS	Sodium Sulfur
SMES	Superconducting magnetic energy storage
SCES	Super Capacitor Energy Storage
SED	Static Economic Dispatch
UR	Upper Reservoir
ZBR	zinc-bromine

Chapter 1. Introduction

1.1. Introduction

This chapter briefly introduces pumped hydro storage (PHS) and the problem investigated in this study. Then, the research's objective, contribution, and thesis structure are presented.

1.2. Overview

Load changes during the day and meeting time-dependent demand, particularly during peak hours, is a significant challenge for energy suppliers. Further, peak demand is growing daily because of the increased end users. Hence, the continuous peak load growth raises the marginal cost of supply. As a result, utilities are concerned about producing power to control or cover peak loads. Power facilities like gas power plants typically cover peak power demand. Diesel generators are also used for supplying isolated power systems during times of peak demand. However, the operating and maintenance (O & M) costs for these kinds of power plants are high. Old and inefficient plants are also used to meet the peak demand because peaking or standby plants only operate during peak load hours. These plants have a low initial cost, but their O & M costs are high. Generally, types of power plants according to purpose can be classified to:

- **Baseload power plants** have *high capital costs but relatively cheap operating costs*, such as large coal-fired plants. These power plants are assigned to supply the baseload of the power system; they are also called “must-run power plants.”
- **Peaking power plants**, such as gas power plants, are inexpensive to build but expensive to operate. They are turned on only during periods of highest demand and have a relatively faster response than baseload power plants.
- **Intermediate load plants**: These plants have characteristics that are somewhere in between and can be quickly ramped up and down.

Considering the above, there is a growing number of research performed on peak shaving, and it is becoming an important area of active research. Further, some countries, such as EU member states and North America, have already deployed this strategy. Peak load shaving is a process of making the load curve flatten by reducing the peak load and shifting it to times of lower demand, Figure 1-1 illustrates the peak

shaving concept. There are different strategies through which peak load shaving can be achieved:

- 1) Integration of Energy Storage System (ESS)
- 2) Integration of Electric Vehicle (EV) into the grid
- 3) Demand Side Management (DSM)

Figure 1-2 illustrates the UAE annual demand curve, specifically in Sharjah City. Among the mentioned strategies for peak shaving, seasonal or annual demand curve flattens cannot be achieved through demand side management or integration of EV alone since the main contribution to peak demand is air conditioning, and this type of load cannot be shifted as it is related to environmental factors. Further, EV integration is not enough due to the high seasonal variation. Therefore, this necessitates the need for long-term and large-capacity ESS to establish a flexible power grid that can respond to seasonal demand fluctuations [1].

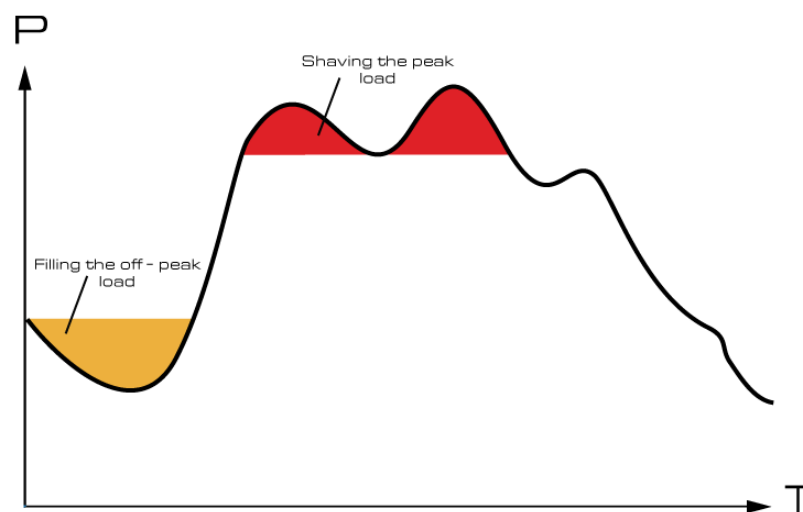


Figure 1-1: Peak Shaving[2]

The flexibility of operation in a power system refers to the built-in buffer between the supply and demand that allow a power system to account for and respond to variability and uncertainty[3]. An energy storage system (ESS) is one of the tools that can provide that buffer as it can charge, hold, and discharge energy according to the grid's condition[4]. There are various ESSs with different capabilities and characteristics. Figure 1-3 summarizes the available ESSs technologies classified under four main categories; mechanical, chemical, Electrochemical, and Electrical storage systems [5]. Understanding different ESSs characteristics is necessary to evaluate their suitability

for different applications. However, a detailed assessment of ESSs is beyond the objective of the research.

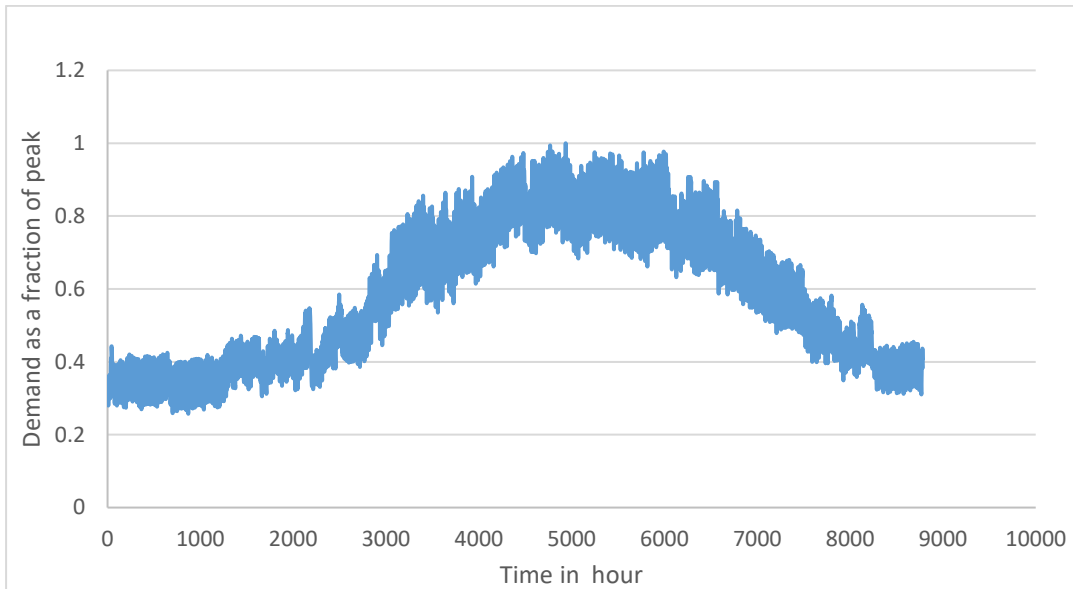


Figure 1-2: UAE annual demand curve

Instead, this section gives a consolidated review of the parameters that would classify an ESS to be suitable for facilitating the high share of renewable energy in the power system or not, a detailed technical assessment of ESSs can be found in [6]. Thereof, only the following parameters compared in Table 1-1 are of essential importance for this objective [7]:

1. Efficiency
2. Capacity range
3. Possible storage duration
4. Energy Volumetric Density

Generally, it can be concluded from the comparison in Table 1-1 that PHS has a relatively high-efficiency range between 70–85% among the long-term ESS and is characterized by a high range of capacities. However, the relatively low energy density of the PHS requires either a large body of water or a large variation in height. For example, 1000 kg of water i.e., $1 m^3$ at the top of a 100m tower has a potential energy of about 0.272 kWh [8]. Therefore, PHS capacity may be practically constrained with limited storage capacity because of their dependency on the geographical location. The main operating principle of PHS is that it deploys potential energy to generate electricity. This is achieved by having two water reservoirs with elevation differences

and a water channel between them, i.e., a penstock. Charging occurs at off-peak periods in which PHS converts electrical energy to potential energy by pumping water from a lower reservoir to an upper one.

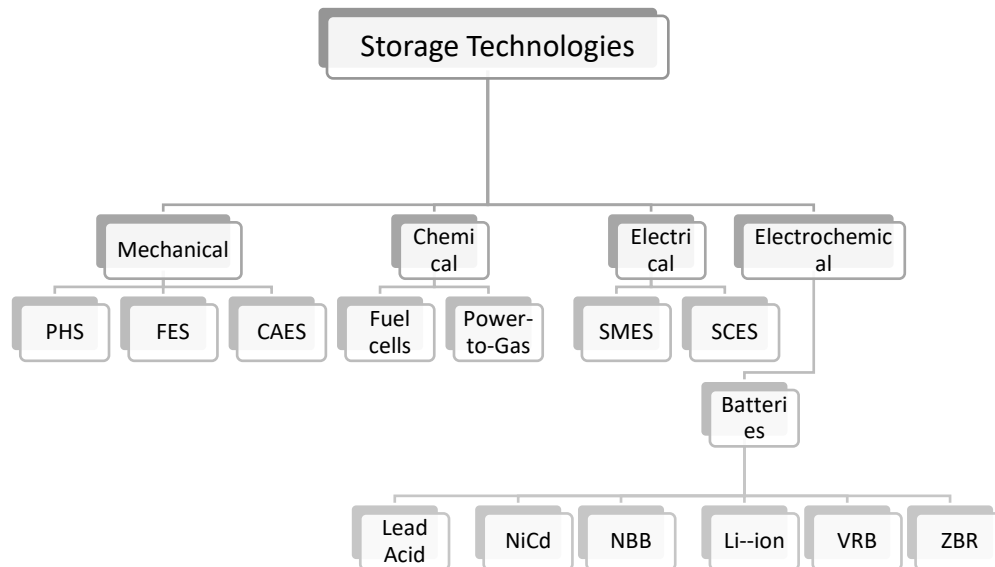


Figure 1-3: Electrical storage technologies

Accordingly, the water in the reservoir at a higher altitude will gain potential energy because it is at a higher position. On the other hand, discharging occurs during peak periods. The water in the high-level reservoir, which is high in potential energy, is allowed to flow through a channel toward the water turbine inlet. The energy of the flowing water arises from the utilization of the potential energy of the reservoir water as it moves down through the penstocks. The use of Bernoulli's equation which is discussed in the next chapter, can explain this process[9] Water movement rotates the turbine runner or impeller, causing mechanical energy; that rotation is eventually converted to electrical energy through a generator coupled with the turbine that feeds the grid[10]. However, despite the geographical challenges, due to the benefits in efficiency, large capacity range, and long possible storage duration, PHS can be considered suitable as a tool to flatten the annual demand curve. Therefore, it is currently the most established technology for controlling energy in the electric power system[11][12]. In this research, we focus on PHS as a tool to increase flexibility in the power grid.

1.3. Thesis objectives

Driven by the necessity to have a long-term and high-capacity energy storage system to flatten the annual demand curve, this thesis aim to optimally manage a PHS unit connected to a conventional grid to assess its performance in supporting the grid on a seasonal basis in the UAE and its associated economic benefits This analysis is essential to motivate the construction of new seasonal PHS plants due to the high construction cost they are identified with, especially in geographical areas where this technology is not yet considered or hard to construct.

1.4. Research contribution

The contributions of this work can be summarized below:

- 1- Establish a framework to analyse and optimally manage the seasonal performance of a grid-connected PHS considering transmission constraints, optimal power flow, and hydraulic model and losses.
- 2- Proposing a methodology that can be adopted in assessing the long-term profitability of PHS utilizing GAMS as an optimization tool.
- 3- Implementing the proposed framework to draw conclusions that would suit the characteristics of the UAE demand pattern which is identified to be high in seasonal variations.

1.5. Thesis organization

Following this introductory chapter, the rest of the thesis is structured into 5 more chapters. Chapter 2 presents the background and related work of the thesis topic, Chapter 3 presents the proposed methodology including the mathematical model, problem formulation, Case study assumptions, and optimization tool. Further, Chapter 4 presents the simulation results and discussion. Finally, Chapter 5 concludes the works and proposes future enhancements.

Table 1-1: Comparison of ESS[12]

Category	Technology		Efficiency%	Capacity rating MW	Time scale	Volumetric Density kW/m ³
Mechanical	PHS		70–85	1–5,000	Hours—months	0.23
	Flywheel		85–95	0.1–20	Seconds—minutes	68-190.
	Compressed air		70–75	50–300	Hours—months	6.9
Electrochemical	Li-Ion		80–90	0.1–50	Minutes—days	270
	Lead-acid		70–80	0.05–40	Minutes—days	75
	Vanadium redox		65–85	0.2–10	Hours—months	125
	Sodium sulfur (NaS)		75–85	0.05–34	Seconds—hours	150
	Nickel-cadmium (NiCd)		65–75	45	Minutes—days	68
	zinc-bromine (ZBR)		60-80	2-10	Hours	0.00745-0.065.
Chemical	Power-to-Gas	Hydrogen	30-75	0.01–1,000	Minutes—months	391
		Methane				1200
Electrical	Superconducting magnetic energy storage (SMES)		85-95	0.01-010	ms-sec	0.00745-0.065.
	(Super Capacitor Energy Storage) SCES		90-97	0.01-0.03	ms-min	125

Chapter 2. Background and Literature Review

This Chapter presents the background information related to the research and the Literature Review of the thesis topic. Hence, some fundamental aspects of PHS are discussed. Further, a brief background on the DC power flow scheme and dynamic economic dispatch (DED) adopted in this research is presented. Finally, we present the related work to the thesis topic.

2.1. PHS fundamentals

This section discusses configurations, elements, power equations, and basic hydraulic terms associated with PHS. Further, Hydro generator types are presented.

2.1.1. PHS configuration

PHS is categorized as a closed or open loop based on its connection to flowing water sources. According to the Federal Energy Regulatory Commission, closed-loop pumped storage is not permanently connected to a naturally flowing water feature, while open-loop pumped storage is [14] PHS plants with closed loops are typically limited to daily or weekly storage cycles because being disconnected from a continuous water source implies limited water input into the system[15]. There have been three different configurations of PHS: a binary set, a ternary set, and a quaternary set, explained below [10]:

- (i) Binary set composed of one reversible pump-turbine unit and one electrical machine (motor/generator)
- (ii) Ternary set composed of one turbine, one pump, and one electrical machine (motor/generator)
- (iii) Quaternary set in which one turbine is driving one generator and one motor for one pump

The earliest PHS in the world appeared in the Alpine regions of Switzerland, Austria, and Italy in the 1890s. The earliest designs used separate pump impellers and turbine generators. Since the 1950s, a single reversible pump-turbine has become the dominant design for PHS [16].

2.1.2. PHS power equation

The potential energy in joules of a mass m located at the top of a dam is represented in (2-1) and (2-2) [17] We can write (2-1) in terms of potential energy difference, as shown in (2-3).

$$PE = F \times h \quad (2-1)$$

$$F = m \times g \quad (2-2)$$

$$E_{max} = \Delta E_{PE} = m \times g \times \Delta h \quad (2-3)$$

where Δh is the elevation difference between two points in meters, F is the force or the weight in Newton, h is the height of the mass from a reference point in meters and m is the mass in Kg , g is the gravitational acceleration in $\frac{m}{s^2}$

Dividing (2-3) by time, we get mass flow rate instead of mass and power instead of energy as in (2-5). Further, the mass flow rate can be written in terms of volume flow rate, where the mass flow rate is equal to the volume flow rate multiplied by the total mass density (2-5) [18] Hence, the PHS power equation can be defined as in (2-4).

$$P = \dot{m} \times g \times \Delta h \quad (2-4)$$

$$\dot{m} = Q \times \rho \quad (2-5)$$

$$P = Q \times \rho \times g \times \Delta h \quad (2-6)$$

However, since we have losses in the system, we don't get the total Energy or power out; it will be reduced by a certain amount depending on the turbine efficiency η_t . Thus, the total energy in Joules stored in PHS and the output power at certain head and flow rate is represented in (2-8) and (2-9) where η_t is the turbine efficiency.

$$E_{stored} = \eta_t \times \rho \times V \times g \times h \quad (2-7)$$

$$P = \eta_t \times Q \times \rho \times g \times \Delta h \quad (2-8)$$

where E_{stored} is the total energy stored in joules, ρ is water density in $\frac{Kg}{m^3}$ and V is the volume in m^3 and P is power in W .

2.1.3. Hydraulic head

Head is a vital element in the PHS energy storage principle. The hydraulic head measures the amount of mechanical energy per unit weight of the fluid. The difference

between the headwater level in the reservoir upstream and the tailwater level in the reservoir downstream determines how much energy can be captured in a PHS planet [19] From the law of conservation of energy, if we can calculate the energy of a flowing liquid at the start of a pipe system point 1, then we know that the same energy must apply at the end of the pipe, point 2, even though the values for each form of energy may have altered. If we ignore energy losses, then we are left with potential energy due to height, potential energy due to pressure, and kinetic energy due to motion.

Potential energy due to height is calculated with reference to some datum level, such as the ground, as stated in equation (2-1) and represented again in (2-9) with the symbol z_1 instead of h . Further, potential energy due to pressure represents the fact that the mass m could rise higher if the pipe were to spring a leak. It would rise by a height of h_1 . where h_1 is given by $h_1 = \frac{P_1}{\rho g}$. and Kinetic energy is calculated as in (2-11) where v the water velocity in $\frac{m}{s}$. Therefore, the total energy of the mass m at point 1 can be given by (2-12).

$$PE_{height} = mgz_1 \quad (2-9)$$

$$PE_{pressure} = mgh_1 \quad (2-10)$$

$$KE = \frac{1}{2}mv^2 \quad (2-11)$$

$$E_1 = mgz_1 + mgh_1 + \frac{1}{2}mv_1^2 \quad (2-12)$$

Similarly, the energy of the same mass at point 2 is given by (2-13).

$$E_2 = mgz_2 + mgh_2 + \frac{1}{2}mv_2^2 \quad (2-13)$$

Therefore, by equating (2-12) and (2-13), cancelling m and divide through by g , we get (2-14)

$$z_1 + h_1 + \frac{v_1^2}{2g} = z_2 + h_2 + \frac{v_2^2}{2g} \quad (2-14)$$

This is known as Bernoulli's equation, after the French scientist who developed it, and is the fundamental equation of hydrodynamics. The dimensions of each of the three terms are the length, and therefore they all have units of meters. For this reason, the

third term, representing kinetic energy, is often referred to as the velocity head. The three terms on each side of the equation are sometimes known as the total head. When carrying out calculations using Bernoulli's equation, it is occasionally helpful to use the substitution $h = \frac{P}{\rho g}$ to change from head to pressure and it is often helpful to use the substitution $v = \frac{Q}{A}$ because the volume flow rate is the most common way of describing the liquid's velocity [20]. Figure 2-1 illustrates Bernoulli's principle, the sum of pressure (potential energy) and kinetic energy is constant i.e., energy is conserved if frictional losses are ignored. Thus, when a fluid flows through areas of different diameters, there is a change in velocity. The change in velocity leads to a change in kinetic energy, so the pressure changes. A decreased pipe diameter means an increase in velocity and kinetic energy and a decrease in pressure [21].

In a pumped hydro storage head is a difference in elevation between the upper and lower water surface levels, which provides the pressure to drive the turbines. Hence, the Hydraulic head can be defined as the height of a static water column above a chosen location, often measured in meters. The hydraulic head or water level at a certain site determines how much energy the water there has[9].

The gross head is the physical elevation difference between these two levels, however, when calculating the output of the plant the net head is used, considering the reduction in pressure due to waterway friction losses and losses at intakes, bends, and changes in waterway section. Pumped storage schemes are designed to minimize these hydraulic losses, which are typically less than 2% of the gross head [22]. Gross head minus head losses equal effective or net head as in (2-15).

$$H_{net} = H_{gross} - H_{loss} \quad (2-15)$$

2.1.4. Hydropower generator

Hydropower generators can be characterized by fixed and variable speeds. The fixed type is a synchronous or induction generator distinguished by a direct grid connection. With this type, hydroelectric or pumped storage installations operate at a constant speed mandated by the synchronous speed of the generator. An induction generator typically experiences a speed variation of 1% to 2%, whereas synchronous generators have no speed variation [23],[24]. The second type is the adjustable-speed generator. One common choice of this type of generator is a doubly fed induction generator

(DFIG). Figure 2-2 (a) illustrates the operating point of constant at synchronous speed hydro turbine, which moves along the dashed line, as the output power is varied by adjusting the wicket gate opening (α). The conversion efficiency of the operating turbine will vary as the output power changes at constant synchronous rotational speed since, for any output power, there will be only a single matching rotational speed that will yield maximum efficiency. On the other hand, Figure 2-2 (b) illustrates the benefits of variable speed operation, which allow the rotational speed and the wicket gate opening to follow the desired output power. Hence, the operating point of the hydro turbine can follow the maximum efficiency.

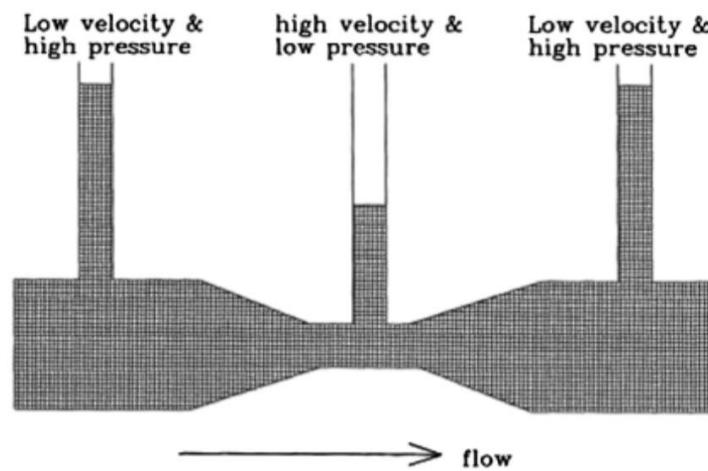


Figure 2-1: Bernoulli Principle

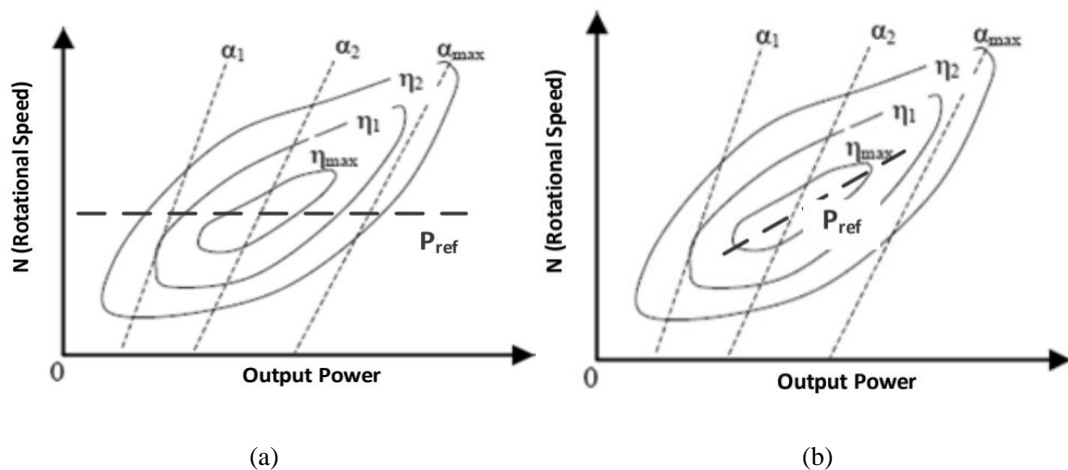


Figure 2-2: illustration of the constant-speed (a) and variable speed operation [24] (b)

2.2. DC power flow

In a specific network, the classic power flow problem consists of active and reactive power flow, and it can be formulated using four variables per node, voltage angle, voltage magnitude, and active and reactive power injections; it finds the power flow in

each line given the load power consumption at all the buses of the electric power system and the generator power production at each power plant[25]. Active power losses are not known in advance as they depend on active power injection patterns and voltage profiles. Other variables are also interdependent, which makes the problem non-linear. The losses are re-estimated at each iteration based on all other variables. This formulation results in a non-linear system of equations that requires iterative solution methods. The decision variables in this problem are generation and voltage level of generating units to minimize the operating costs[26], [27]. DC power flow estimates lines power flows on AC power systems, addresses the active power calculation, and neglects reactive power flows. It neglects active power losses and assumes that magnitudes of nodal voltages are equal. The voltage magnitudes are approximately 1 pu. Furthermore, voltage angle differences are assumed to be small [26].

The only variables are voltage angles θ and active power injections. However, all active power injections are known in advance since losses are neglected. Therefore, the problem becomes linear, and there is no need for iterations. For each node in the system. It is non-iterative and convergent. The angle of the slack bus is assumed to be zero as the reference for the rest of the network.[27]. We choose DC power flow in this research since we require a repetitive fast load flow estimation as we are doing dynamic economic dispatch (DED) over a relatively long period. The dynamic economic dispatch will be discussed in the next section. DC power flow is categorized with an excellent robust, reasonable Convergence rate, adequate accuracy, and low CPU requirements [25].

2.3. Dynamic economic dispatch

Power system dispatch can be classified into two categories one is static dispatch and the other is dynamic dispatch. Static economic dispatch (SED) searches for the optimal solution in each separated period without taking the relationships among different periods into account hence revealing results for demand for a particular time [25]. The static dispatch does not look ahead over the future time horizon, using predicted load trends (i.e., 1-2 hours ahead), the input load data, is a smoothed estimate of the present load [25], [28][26]. Hence, given a network of power generators, the SED problem is concerned with finding how much power each unit should generate to serve a particular area to meet the load while minimizing the total operational costs. and the on and off status of units is assumed to be known [29]. On contrary, DED refers to dispatch a set

of units over a given operating horizon. It determines the optimal scheduling of online generator outputs with predicted load demands over a certain period [30]. It considers the coupling in the time domain; for example, it includes ramp rate constraints for generators and prohibited operating zones [31][32],[30]. Both dynamic and static economic dispatch (ED) can be further subdivided into convex and nonconvex problems based on the convexity on the basis of the fuel cost function. In Convex problem, the fuel cost function is a quadratic function of the generator coefficients as will be presented in (3-25) in Chapter 3, [32]

This formulation for operating cost is the most common formulation in ED problems because this function is convex and guarantees a globally optimal solution [33] However, the objective function in certain practical ED problems may be nonlinear and non-convex [34]. It is worth mentioning that unit commitment determines the on and off status, i.e., which units are available for dispatch. we assume unit commitment to be performed apart from the economic dispatch and not considered in this research. It also would deal with many other global considerations. for example, the start-up and shutdown costs, maintenance schedules, and power purchase and sell agreements [35]. Hence, ED is the problem of scheduling the output power levels of the committed (online) generating units in a power system [36],[25],[28].

The DED, in isolation, calculates how much power is produced at each power generator, ignoring the transmission network. On the other hand, the basic power flow problem calculates how much power should be sent around a network at one snapshot in time and it ignores how that power is produced. combining both yield Optimal Power Flow (OPF) which solves the ED problem with the inclusion of Network constraints [37].

2.4. Literature review

The research field is rich with numerous studies in all possible aspects in which PHS can support the grid, such as tracking and adapting to drastic load changes, modulating the frequency, maintaining voltage stability, providing reserve generation and economic benefits. As well as grid balancing when distributed energy resources are integrated[8]. The literature review is primarily constructed on references that have studied PHS operation from an economic optimization perspective. The references have

been evaluated and critiqued and at the end of this section, to highlight where this work stand in the field.

In [38], an energy dispatch model was presented for a hybrid system of 4 four components: PV unit, wind unit, pumped hydro storage system and a diesel generator. The paper considered the intermittent nature of the distributed energy resources as well as the variations in demand. The objective of the study was to minimize the cost function of the hybrid system while optimizing the system's power flow considering different operational constraints of the four components. The simulations have been performed in MATLAB using Fmincon. The developed model has been applied to two use cases; the simulation results are analysed and compared to the conventional case when the diesel generator is the only source to supply the given load demand. The results proved that the developed control model for the proposed hybrid system achieved more savings. In [39], the study used a technique called social group entropy optimization (SGEO) to solve fuel-constrained dynamic economic dispatch (FCDED) with demand side management (DSM) integrating renewable energy sources and pumped hydro storage plant. The dynamic economic dispatch (DED) is performed in two cases: with fuel contains and without fuel constrains. Test results show that fuel consumption can be sufficiently controlled for fulfilling constraints imposed by suppliers. The entire scheduling period is 1 day and segregated into six intervals each containing 4 h.

In [40] an improved probabilistic production simulation method with sequential load correction scheme is developed to capture the time-dependent features of pumped hydro storage and renewable energy generation. A pumped storage scheduling is used to mitigate the imbalanced power that is caused by the intermittence nature of the distributed energy resources. Hence, the objective function can be defined as the minimization of cumulative imbalanced energy during the scheduling horizon. In [41], individual scheduling of PHS plants is studied using Dynamic programming. UCP of thermal generating units. The model was tested against 2 PHS plants placed in IEEE 30 bus system, over 24 hours scheduled horizon. As a result, a suitable location of the PSH plants in IEEE 30 bus system is suggested. In [42], a new stochastic optimization framework for a day-ahead (DA) energy management in renewable-based isolated rural microgrid. The proposed microgrid system involved non-dispatchable distributed generations (DGs) like a wind unit and a photovoltaic (PV) unit to supply the

consumer's demand. Maintaining a balance between generation and demand. Therefore, a pumped-storage unit and an incentive-based demand response program have been used in this work to cope with this challenge. Moreover, the responsive demand and distribution network as well as the inherent uncertainty of wind and PV power generation have been considered in this paper. The results proved that the optimal scheduling and demand response implementation of the pumped-storage unit have significantly improved economic and technical performance indexes.

In [43], an optimization framework for optimal operation of a hybrid system is presented. The system is built in MATLAB and is composed of PV, diesel generator and PHS. The optimization technique used in this work is a modified crow search algorithm (CSA) with the fuel consumption as the objective function. As stated by the author, the outcomes of the proposed technique outperformed genetic algorithm (GA), particle swarm optimization (PSO) and original CSA models from accuracy and robustness perspective. Moreover, optimal sharing of deficit power between diesel generator and PHS leads to having minimum operation cost. the optimization was done for a duration of 24 hours. In [44], a framework based on reinforced learning is proposed to learn an optimal decision policy for online intelligent economic dispatch. The study was done on a hybrid hydro/PV/PHS system considering both the economic benefit and power fluctuation. More than 600 days of hourly data are selected as training samples while 3 consecutive days are selected as test Data. In [45] chaotic fast convergence evolutionary programming (CFCEP) was used for solving intricate actual world combined heat and power dynamic economic dispatch (CHPDED) problem using MATLAB. The model involved demand side management (DSM) incorporating renewable energy sources and pumped-storage-hydraulic unit. Dynamic economic dispatch was performed on a duration of 24 hours. In [46], a concept of small isolated electric power generation from PHS using wind as primary energy is proposed for rural and remote areas. A suitable well is utilized as the lower reservoir of the PHS system, while the upper reservoir (UR) needed for the water storage is made on the ground. For validation, the simulation was carried out for a course of 24 hours. The simulated results matched the designed system.

In [47] In this paper, a medium to long-term optimal operation strategy is proposed for independent regional power grid in the dry season based on the statistical characteristics of wind-solar power and the long-term plan of hydropower. The objective of the work

is to minimize the difference between the monthly water consumption of hydropower stations and the predicted, considering the constraints of water flow and daily average battery energy storage fluctuation.

In [48] the impact of intermittent wind generation, coupled with a given hydro capacity, on wholesale electricity prices, accounting for both spatial and seasonal effects was investigated. The author state that during dry seasons, when hydro storage is low, and the wind resource is insufficient, relatively more expensive thermal generation is required to satisfy demand, which increases price volatility. The findings suggest that one option is to expand wind generation in sites complementary to hydro generation and the other is pumped hydro storage which also could help reduce price volatility and maintain grid stability,

In [49], A solution to help in planning and decision-making for hydropower producers maximize the profit in the electricity market considering the optimal operation of power plants. A dynamic production profitability model has been developed. The model used in this research leveraged the principles of System Dynamics to simulate hydroelectric systems under different scenarios to evaluate the performance of the hydropower generation system. Using STELLA software, which is an object-oriented simulation environment, the profitability prediction mechanism was developed by utilizing historical data of 10 years to perform the prediction over the course of 24 months. The forecasted profit in each scenario of the hydroelectric plant has been discussed

Although pumped hydro storage may be seen as a strategic key asset by grid operators and despite the benefits it can add to the grid, financing PHS project is a concern as it has high investment cost. Therefore, and reference to the reviewed literature, it has been observed that there is a lack in PHS long term profitability analysis.

The more efforts invested to understand the commercial aspects of PHS, the more guarantees will be established for the payment of the capital cost and a clearer rate of return and hence would motivate constructing new PHS plants especially for geographical areas which are not yet identified by the availability of pumped hydro or where it is difficult to find naturally suitable sites close to large water resources, with reasonable height difference between the lower and upper reservoir. This work is proposing a framework to analyse and optimally manage the performance of a seasonal grid connected PHS unit considering transmission constraints, optimal power flow, and

hydraulic model and hydraulic losses, in which it can be adopted for one year profitability assessment utilizing GAMS as optimization tool. Further, the proposed framework is implemented to draw conclusion that would suit the characteristics of UAE demand pattern which is identified to be high in seasonal variations.

Chapter 3. Methodology

In this chapter, we present the methodology illustrated in Figure 3-1. First, we build the mathematical model and formulate the proposed optimization problem. Further, the case study, including data collection, preparation, and assumptions to establish the input to the optimization problem, is presented; this includes consumption data, thermal generation units' technical data and cost function coefficients, transmission lines power limits, and technical parameters, and PHS unit parameters. Finally, the optimization tool is discussed.

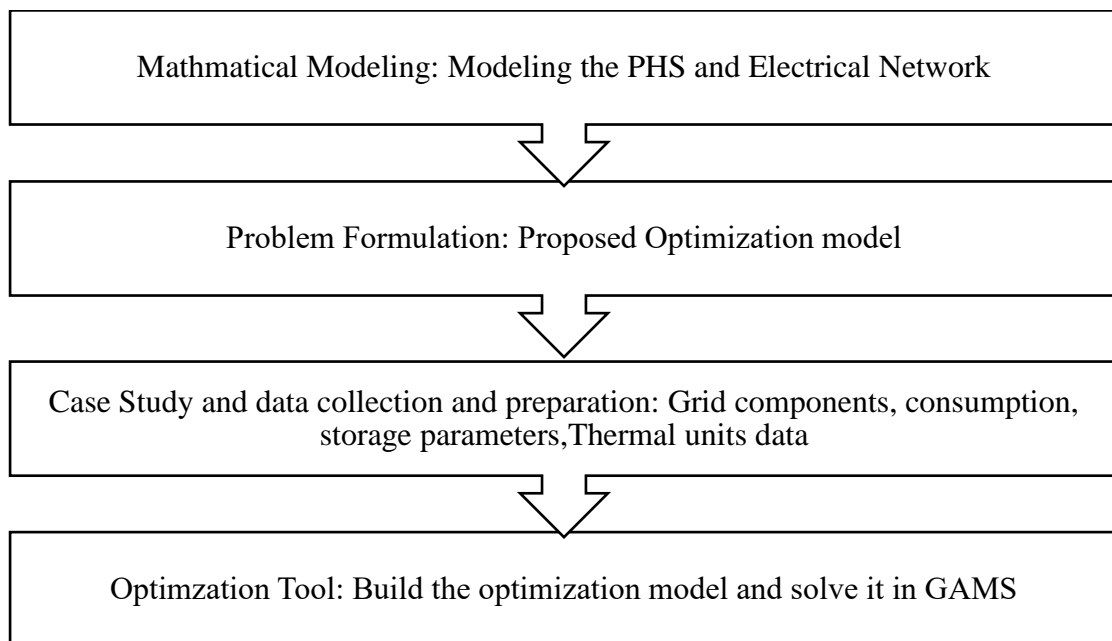


Figure 3-1:Proposed Methodology

3.1. Network mathematical model

This section introduces the multi-period mathematical model of the proposed system, the subscript t denotes the time in hours and the subscript d denotes days. The time step is considered as one hour.

3.1.1. PHS unit model

PHS system has four main elements: pipes or penstock, the pump, the upper and lower reservoirs, and the hydro turbine. In this section, we present the mathematical model of the four elements.

3.1.1.1. Penstock

Pipes or penstock's primary objective is to convey water as it moves from one point to another. However, while water is transported its energy is dissipated in pipes due to friction, which is translated in water head losses. Hydraulic head losses are expressed in meters. Several equations in literature are used to describe friction head loss along a pipe. We choose Darcy-Weisbach in this research [50]. The head loss equation is presented in (3-1), where R is the hydraulic resistance of the pipe H_{losses} is head loss in m and Q is the flow in $\frac{m^3}{s}$.

$$H_{d,t}^{loss} = RQ_{d,t}^2 \quad (3-1)$$

$$R = K \cdot \frac{8}{\pi^2 \cdot D^4 \cdot g} \quad (3-2)$$

$$K = K_{pipe} + K_{fitting} \quad (3-3)$$

$$K_{pipe} = \frac{f \cdot L_p}{D_p} \quad (3-4)$$

$$f = [1.8 \log(\frac{6.9}{Re} + (\frac{\varepsilon/D}{3.7})^{1.11})]^{-2} \quad (3-5)$$

$$Re = \frac{\rho v D}{\mu} \quad (3-6)$$

$$v = \frac{Q}{A} \quad (3-7)$$

$$v = \frac{Q}{0.25 \cdot \pi \cdot D^2} \quad (3-8)$$

K represents the total resistance coefficient which consists of the resistance coefficient of the pipe K_{pipe} and resistance coefficient of the pipe fittings $K_{fitting}$. The resistance coefficient of the pipe K_{pipe} is a function of the friction factor f while $K_{fitting}$ depends on the pipe fittings material and D is the pipe diameter.

f is the dimensionless Darcy-Weisbach friction factor, which is a function of the Reynolds number, denoted Re and $\frac{\varepsilon}{D}$ is the relative roughness where ε in mm is the absolute roughness and it depends on the pipe material. The friction factor f in Darcy-Weisbach can be determined from the Moody diagram or by solving the Colebrook-White equation. There is in the literature a number of formulas that approximate the Darcy friction coefficient f , we used equation (3-5) this equation is derived from the Moody chart to approximately calculate the friction factor f . The Reynolds number Re is a dimensionless number used to categorize the fluids systems in terms of flow pattern

of a fluid also μ is dynamic viscosity of water which is a constant 8.90×10^{-4} Pa·s at about 25 °C and ρ is the water density in $\frac{\text{Kg}}{\text{m}^3}$ and it is 997 at 25 °C and v is the water velocity in $\frac{\text{m}}{\text{s}}$. Head loss can be calculated using equation (3-1) [51]. Equations (3-2) to (3-8) are concerned with calculating the hydraulic resistance of the pipe. Practically, the hydraulic resistance value is variable and depend on the friction factor, which is in turn a function of Reynolds number, denoted R_e . Reynolds number depends on the velocity of the flow at a specific time. However, the friction losses and Hydraulic resistance was estimated in this research and assumed constant. From the previous equations, it's evident that the hydraulic resistance of the pipe is directly proportional to the pipe length. Hence it is recommended to reduce the vertical and horizontal distance of the penstock

3.1.1.2. Pump model

The pump model calculates the pump flow rate $Q_{d,t}^p$ as a function electrical power input to the motor driving the pump P_m . Equation (3-9).

$$Q_{d,t}^p = \phi(P_{d,t}^m) \quad (3-9)$$

For an electrically driven motor, the input power P_m is the total electrical power supplied to the pump system, i.e., to the electrical motor. Output power is the mechanical power at the pump shaft $P_{d,t}^p$ to elevate the water from the lower reservoir to the upper reservoir. The difference between $P_{d,t}^m$ and $P_{d,t}^p$ comes from the motor's efficiency η_m . The more efficient the motor is, the less power is lost converting from electrical power to mechanical power. The motor efficiency accounts for both the mechanical and electrical losses of the motor. Where η_m is a function of P_m . However, in this research, we consider the motor efficiency constant. Thus, the mechanical power at the pump Shaft or output of the motor can be modeled in (3-10). Further, pump output flow rate $Q_{d,t}^p$ is a function of $P_{d,t}^p$ and is represented in (3-11).

$$P_{d,t}^p = P_{d,t}^m \cdot \eta_m \quad (3-10)$$

$$Q_{d,t}^p = \frac{P_{d,t}^p \eta_p}{\rho \cdot g \cdot H_{d,t}^p} \quad (3-11)$$

where η_p is the pump efficiency and is a function of $Q_{d,t}^p$. However, in this research, we consider the η_p constant. The pump should be able to provide at any time step an $H_{d,t}^p$ that is not less than the expected hydraulic head losses $H_{d,t}^{loss}$ which is calculated as clarified in the penstock section and the static head $H_{d,t}^s$ which is defined as the total distance from the water surface in the lower reservoir to the water surface in the upper reservoir. Accordingly, the static head changes as the water levels changes in both the lower and upper reservoirs [22]. Hence, the total pump delivered head $H_{d,t}^p$ modeled as in (3-12). Reference to (3-1), pump head loss $H_{d,t}^{p,loss}$ can be modeled as (3-13)

$$H_{d,t}^p = H_{d,t}^s + H_{d,t}^{p,loss} \quad (3-12)$$

$$H_{d,t}^{p,loss} = RQ_{d,t}^p{}^2 \quad (3-13)$$

$$H_{d,t}^s = h_z + l_{d,t-1} \quad (3-14)$$

In this research we have assumed a fixed lower reservoir level which is a water source and a variable UR level, a human made tank. $H_{d,t}^s$ consists of fixed and variable parts since there is a fixed vertical distance between the two reservoirs and the variable part is due to the fact that the UR water level changes as the tank is being filled or emptied. $H_{d,t}^s$ can be hence calculated as in (3-14), where h_z is the fixed vertical elevation between the two reservoirs and $l_{d,t-1}$ is water level in the UR before pumping occurs, therefore time subscript is reduced by 1.

3.1.1.3. UR model

The UR model is a dynamic modeling of the water level in the reservoir due to the increment or decrement by the pumping or turbine process and can be represented as in (3-15).

$$l_{d,t} = l_{d,t-1} + \left(\frac{Q_{d,t}^p - Q_{d,t}^{tur}}{A} \right) \cdot \Delta T \quad (3-15)$$

where $Q_{d,t}^{tur}$ is the turbine flow rate in case of discharging and $Q_{d,t}^p$ pump flow rate in case of charging. A is the cross-sectional area in m^2 of the tank, $l_{d,t-1}$ is previous level of the tank and ΔT is the time interval in hour.

3.1.1.4. Turbine model

The turbine model calculates the output power $P_{d,t}^{tur}$ of the turbine as a function of the flow rate $Q_{d,t}^{tur}$ and the turbine head $H_{d,t}^{tur}$. equation (3-16) and (3-17) .

$$P_{d,t}^{tur} = \phi(Q_{d,t}^{tur}, H_{d,t}^{tur}) \quad (3-16)$$

$$P_{d,t}^{tur} = n_t \cdot \rho \cdot Q_{d,t}^{tur} \cdot g \cdot H_{d,t}^{tur} \quad (3-17)$$

Reverse to the pump operation, the mechanical energy is converted into electrical energy. The efficiency of the turbine n_t reflect how much energy is lost due to mechanical losses in the turbine and how much is converted into electrical energy, and it is a function of turbine flow [51]. However, in this research the turbine efficiency is assumed constant, where $H_{d,t}^{tur}$ is the net head driving the turbine at specific time step. Net head is defined as the actual water pressure driving the turbine after deduction of friction losses in the waterway but adding back the kinetic energy of the water flow based on the explained Bernoulli principle in Chapter 2. Mathematically, net head can be presented as gross static head minus the head losses. In this study we are assuming the turbine to be a Francis turbine type which can operate in either pumping or turbine mode, in which gross static head is defined as distance from the water surface in the lower reservoir to the water surface in the UR which is the same definition of the static head in the previous section $H_{d,t}^S$ [22] Hence, the turbine net head $H_{d,t}^{tur}$ equal static head minus the head loss $H_{losses,t}$ along the penstock Equation (3-18). Reference to (3-1), pump head loss $H_{d,t}^{p,loss}$ can be modeled as

$$H_{d,t}^{tur} = H_{d,t}^S - H_{d,t}^{t,loss} \quad (3-18)$$

$$H_{d,t}^{t,loss} = RQ_{d,t}^{tur2} \quad (3-19)$$

3.1.2. DC power flow model

Based on technical background given in Chapter 2, to construct a DC power flow model, the below assumptions have to be considered:

- 1- Line resistances (active power losses) are negligible i.e., $R \ll X$.
- 2- Voltage angle differences are assumed to be small i.e., $\sin \theta = \theta$ and $\cos \theta = 1$.
- 3- Magnitudes of bus voltages are set to 1.0 per unit (flat voltage profile).

It is worth to mention that DC power flow is a variation of the Newton–Raphson method hence, reflecting the above assumptions equation (3-20) that represent AC active power flow used in Newton–Raphson method, can be reduced to equation(3-24) resulting in a formulation between P and θ . Hence voltage angles and active power injections are the variables of DC power flow Problem. Equations (3-21), (3-22) and (3-23) reflect assumption 1,2 and 3 in the above list respectively, where P_i is the injected power at bus i . in which B_{ij} is susceptance of the transmission line, and for any given transmission circuit with impedance of $Z = R + jX$, will have an admittance of $Y = G + jB$. Since the Line resistances (active power losses) are negligible, B_{ij} will be the reciprocal of the reactance X_{ij} between bus i and bus j . As a result, active power flow through a transmission line, between buses i and j at time t and day d can be formulated

$$P_i = |V_i| \sum_{j=1}^n |V_j| [G_{ij} \cos(\theta_i - \theta_j) + B_{ij} \cdot \sin(\theta_i - \theta_j)] \quad (3-20)$$

$$P_i = \sum_{j=1}^n B_{ij} \cdot \sin(\theta_i - \theta_j) \quad (3-21)$$

$$\sin(\theta_k - \theta_i) = (\theta_k - \theta_i) \quad (3-22)$$

$$P_i = \sum_{j=1}^n [B_{ij} \cdot (\theta_i - \theta_j)] \quad (3-23)$$

in (3-24), where $X_{d,t}^{ij}$ is the reactance of line ij , $\theta_{d,t}^i - \theta_{d,t}^j$ is Voltage angle differences and $P_{d,t}^{ij}$ is the power flow between buses i and j .

$$P_{d,t}^{ij} = \frac{\theta_{d,t}^i - \theta_{d,t}^j}{X_{d,t}^{ij}} \quad (3-24)$$

3.1.3. Dynamic economic dispatch

In this research we are using cost-based DED problem. and a convex cost function for simplicity.[26] The production costs of a thermal unit are defined as in equation (3-25) where a_g , b_g , and c_g are the fuel cost coefficients of the j th unit.

$$Cost = \sum_g a_g (P_{d,t}^g)^2 + b_g (P_{d,t}^g) + c_g \quad (3-25)$$

In this research we only considered coupling in time domain through Ramp rates constraints equations (3-26) and (3-27). It basically states what is the maximum possible change in a unit output over a period, where RU_g represents upper ramp rate

limit of generators when generation must be increased due to increase in load and RD_g represents down ramp rate limit of generators when generation must decrease due to decrease in load, $P_{g,t}$ is the current generation of the unit and $P_{g,t-1}$ is previous generation of the unit [32]. In addition, the operational constraints on the thermal units are in (3-28).

$$P_{d,t}^g - P_{d,t-1}^g \leq RU_g \quad (3-26)$$

$$P_{d,t-1}^g - P_{d,t}^g \leq RD_g \quad (3-27)$$

$$P_g^{min} \leq P_{d,t}^g \leq P_g^{max} \quad (3-28)$$

3.1.4. Problem formulation

In this section we formulate the proposed optimization problem which combine the network power flow, DED and PHS unit. The optimization problem decision variables and state variables are defined in Table 3-1. The objective function:

The objective function is the DED thermal generation units cost function. (3-25) unless that it will be multiplied by 90 to account for the full season as in (3-30). The operation cost should be minimized over the study period, where g is index of thermal generating

$$P_{d,t}^{gen} = [P_{d,t}^1 \quad P_{d,t}^i \quad \dots \quad P_{d,t}^n \quad P_{d,t}^p \quad P_{d,t}^{tur}]^T \quad (3-29)$$

units. Real power output of the corresponding thermal generator units and the PHS unit are optimized according to objective

$$Min \quad Cost = \sum_{d,t,g} 90 \times \{a_g(P_{d,t}^g)^2 + b_g(P_{d,t}^g) + c_g\} \quad (3-30)$$

. An illustration to the proposed system configuration is presented in Figure 3-2. The decision variable vector $P_{d,t}^{gen}$ is represented in (3-29), where n is the number of the thermal units to be scheduled within the network i.e. the 12 in addition to $P_{d,t}^p$ and $P_{d,t}^{tur}$ related to BHS unit.

1- The objective function:

The objective function is the DED thermal generation units cost function. (3-25) unless that it will be multiplied by 90 to account for the full season as in (3-30). The operation cost should be minimized over the study period, where g is index of thermal generating units. Real power output of the corresponding thermal generator units and the PHS unit are optimized according to objective

$$\text{Min Cost} = \sum_{d,t,g} 90 \times \{a_g(P_{d,t}^g)^2 + b_g(P_{d,t}^g) + c_g\} \quad (3-30)$$

2- Equality constraint.

- Power balance equation (3-24) and Equation (3-31);this implies that power balance between generation, demand and power transfers should be satisfied in all time steps. Noting that $P_{d,t}^{tur}$ and $P_{d,t}^p$ are with positive and negative signs respectively to refelct the charging and discharging of PHS unit.

$$\sum_{g \in \Omega_G^i} P_{d,t}^g + P_{d,t}^{tur} - P_{d,t}^p - P_{d,t}^d = \sum_{j \in \Omega_l^i} P_{d,t}^{ij} \quad (3-31)$$

where:

j,i index of Network buses

Ω_g set of all thermal generating units

Ω_G^i set of all thermal generting units connected to bus i

Ω_l set of Network branches

Ω_l^i set of all busses connected to bus i

$P_{d,t}^d$ demand

- Pump and turbine power equations (3-11) and (3-17)
- Pump and turbine head equations (3-12) and (3-18)
- Pump and turbine head loss equations (3-13) and(3-19)
- Water level in the UR equation (3-15)
- UR initial value at the beginning of each season. (3-32)to(3-35)

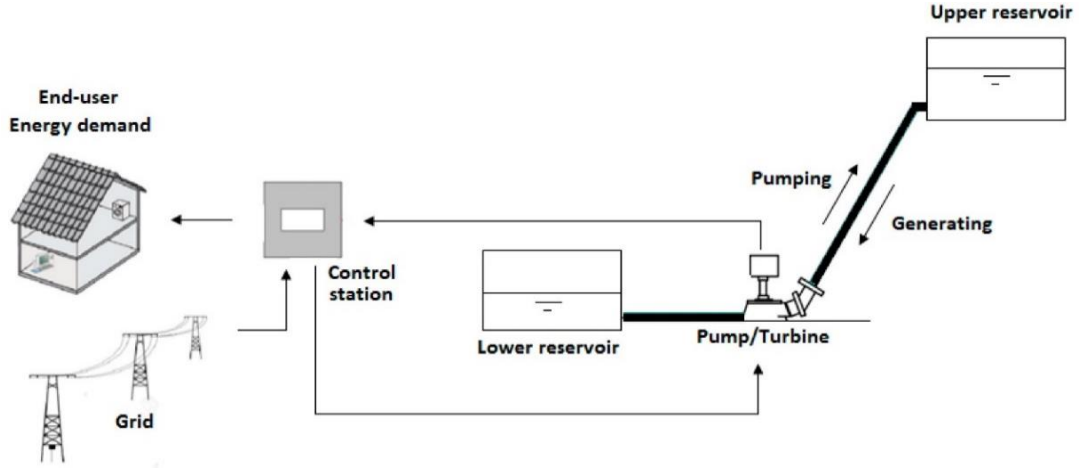


Figure 3-2:Proposed system Diagram[52]

In addition to the equality constraints on the water level in the upper reservoir, four more equations are included in the model to link the initial values in the UR at beginning of each season to the previous season. Each season is approximated as one day as stated previously. Therefore, the difference between the water level in the last hour i.e., 24 from a specific day representing a specific season and the initial value of the same day multiplied by 90 and added to the initial value of the same day should be equal to the initial value of the UR level of the next day, i.e., season.

$$l_2^i = l_1^i + 90 \times (l_{1,24} - l_1^i) \quad (3-32)$$

$$l_3^i = l_2^i + 90 \times (l_{2,24} - l_2^i) \quad (3-33)$$

$$l_4^i = l_3^i + 90 \times (l_{3,24} - l_3^i) \quad (3-34)$$

$$l_1^i = l_4^i + 90 \times (l_{4,24} - l_4^i) \quad (3-35)$$

3- Inequality constraints:

- Ramp up and ramp down constraints represented in (3-26) and (3-27)
- Thermal units operating limits specified in equation (3-28).
- Network transmission line limits represented in equation (3-36),
- Pump and Turbine power limits (3-37) and (3-38)
- Flow minimum limits, However, maximum limits is constrained with the pump and turbine maximum power limits.(3-39) and (3-40)
- UR maximum and minimum limits (3-42)
- UR initial value maximum and minimum limits(3-42)
- Voltage angle limits (3-43)

$$-P_{ij}^{max} \leq P_{d,t}^{ij} \leq P_{ij}^{max} \quad (3-36)$$

$$P_{d,t}^{min} \leq P_{d,t}^{tur} \leq P_{d,t}^{max} \quad (3-37)$$

$$P_{d,t}^{min} \leq P_{d,t}^p \leq P_{d,t}^{max} \quad (3-38)$$

$$Q_{d,t}^{t,min} \leq Q_{d,t}^t \quad (3-39)$$

$$Q_{d,t}^{p,min} \leq Q_{d,t}^p \quad (3-40)$$

$$l_{d,t}^{min} \leq l_{d,t} \leq l_{d,t}^{max} \quad (3-41)$$

$$l_{d,t}^{min} \leq l_d^i \leq l_{d,t}^{max} \quad (3-42)$$

$$\theta_{d,t}^{min} \leq \theta_{d,t}^i \leq \theta_{d,t}^{max} \quad (3-43)$$

Table 3-1: Optimization Problem Variables

Decision Variable	Definition	State Variable	Definition
$P_{d,t}^p$	<i>Pumping Power</i>	l_d^i	<i>Initial Level of upper reservoir</i>
		$l_{d,t}$	<i>Water level in upper reservoir</i>
$P_{d,t}^g$	<i>Thermal Unit Power</i>	$H_{d,t}^{p,loss}$	<i>Hydraulic losses in pumping mode</i>
		$H_{d,t}^{t,loss}$	<i>Hydraulic losses in turbine mode</i>
$P_{d,t}^{tur}$	<i>Turbine Power</i>	$Q_{d,t}^p$	<i>Pumping flow</i>
		$Q_{d,t}^{tur}$	<i>Turbine flow</i>
		$H_{d,t}^p$	<i>Head in pumping mode</i>
		$H_{d,t}^{tur}$	<i>Head in trubine mode</i>
		$H_{d,t}^s$	<i>Static head</i>
		$P_{d,t}^{ij}$	<i>Power flow in line ij</i>
		$\theta_{d,t}^i$	<i>Voltage angle</i>

3.2. Case study: data collection and preparation

This section presents the data and assumptions considered in this research.

3.2.1. Study period and demand data

PHS performance is expected to vary throughout the year due to seasonal variations in electricity demand. Hence, the study period of one year to monitor the effect of seasonal variation on charging and discharging decisions was considered over a time step of one

hour. A one-year demand figure was retrieved from SEWA and divided into four quarters, each of approximately 90 days, in which each quarter represents a season. Hence, the average demand of the same hour of each day in the same season was calculated, i.e., we ended up with demand data of 4 days and 96-time steps. The demand data of the 96-time steps is given in Appendix A. This representation of the study period is done to ensure a manageable simulation time.

3.2.2. 24bus-IEEE RTS bus system

This research utilises the 24-bus IEEE Reliability Test System (RTS), a transmission network with voltage levels of 138 kV, 230 kV, and $S_{base} = 100MV$. The Electrical network is shown in Figure 3-3 and modified to integrate a PHS unit at bus 19. The Network is structured using the transmission lines' power limits, technical parameters, and connection details, in Table 3-2, and using the generating units' data and connection details, as presented in

Table 3-3. The data was retrieved from [26], with modifications. There are 12 Thermal generating units connected to different buses, in which the sum of the maximum possible output of all units is 3375MW. The slack bus is bus 13. The load is connected to buses as per Table 3-4. The maximum possible demand for all buses is, at most 2850MW.

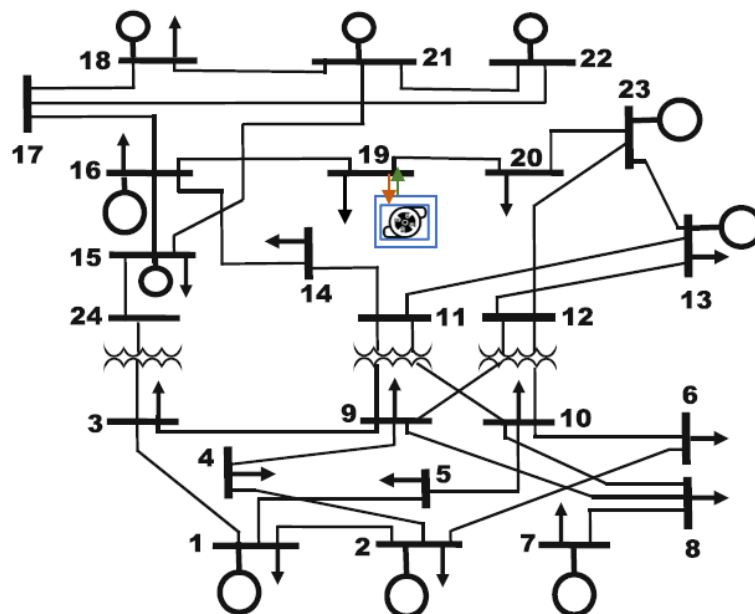


Figure 3-3 proposed IEEE24 bus system with PHS unit at bus 19

Table 3-2: IEEE RTS 24-bus system branch data

From	To	b(pu)	Rating (MVA)	From	To	b(pu)	Rating (MVA)
1	2	0.4611	175	11	13	0.0999	500
1	3	0.0572	175	11	14	0.0879	500
1	5	0.0229	175	12	13	0.0999	500
2	4	0.0343	175	12	23	0.203	500
2	6	0.052	175	13	23	0.1818	500
3	9	0.0322	175	14	16	0.0818	500
3	24	0	400	15	16	0.0364	500
4	9	0.0281	175	15	21	0.206	1000
5	10	0.0239	175	15	24	0.1091	500
6	10	2.459	175	16	17	0.0545	500
7	8	0.0166	175	16	19	0.0485	500
8	9	0.0447	175	17	18	0.0303	500
8	10	0.0447	175	17	22	0.2212	500
9	11	0	400	18	21	0.109	1000
9	12	0	400	19	20	0.1666	1000
10	11	0	400	20	23	0.091	1000
10	12	0	400	21	22	0.1424	500

Table 3-3: Thermal Generating units' data

Gen	Bus	P_i^{max} MW	P_i^{min} MW	a_i (\$/MW ²)	b_i (\$/MW)	c_i (\$)	RU(MW/h)	RD(MW/h)
g1	18	400	90	117.7	5.47	0.02533	47	47
g2	21	420	100	117.7	5.47	0.01199	47	47
g3	1	152	30.4	100	13.32	0.005	14	14
g4	2	152	30.4	660	13.32	0.00413	14	14
g5	15	155	54.25	300	16	0.0025	21	21
g6	16	155	54.25	81	10.52	0.00876	21	21
g7	23	310	108.5	500	10.52	0.002	21	21
g8	23	350	140	500	10.89	0.00623	28	28
g9	7	350	75	217	20.7	0.00211	49	49
g10	13	591	206.85	680	20.93	0.02533	21	21
g11	15	60	12	680	26.11	0.01199	7	7
g12	22	300	0	100	26	0.005	35	35

Table 3-4: Demand Details

Bus	P_d MW
1	108
2	97
3	180
4	74
5	71
6	136
7	125
8	171
9	175
10	195
13	265
14	194
15	317
16	100
18	333
19	181
20	128

3.2.3. PHS unit assumptions and parameters

This section presents the technical parameters and assumptions considered for the PHS. This research assumes that the PHS configuration is a one-unit configuration hosted in a powerhouse, a reversible pump turbine coupled to a reversible motor generator. The parameters considered for both modes will be discussed

3.2.3.1. Lower reservoir

A lower reservoir is assumed to be a water source at sea level, with a fixed water level acting as a reference point to the system.

3.2.3.2. Upper reservoirs

The UR is assumed to be above the lower reservoir by h_z equal to 210 m, the assumed cross-sectional area is 25510 m^2 , and the reservoir height is 90 m. Previously defined (2-7) can be used to calculate the storage volume V_s substituting by h_t the total head and the desired storage capacity; the tank is assumed to have a cylindrical-shaped, (3-44) and (3-45) define h_t and A the cross sectional area of the upper reservoir, where

h_s is the maximum possible storage height, i.e. when the storage is full. Figure 3-4 is a graphical illustration of storage parameters.

$$h_t = h_s + h_z \quad (3-44)$$

$$A = \frac{V_s}{h_s} \quad (3-45)$$

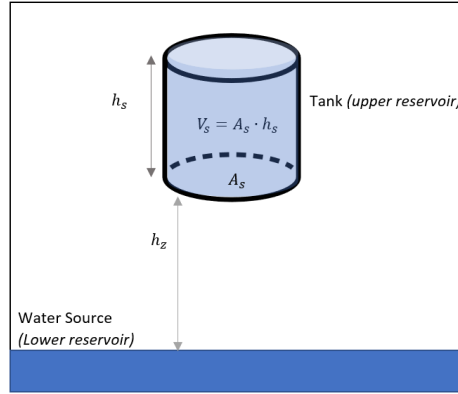


Figure 3-4: PHS unit Energy Capacity Parameters

3.2.3.3. Storage cycle

The proposed PHS unit is intended to be simulated as seasonal storage. Hence, the unit is expected to store and reach the rated storage capacity, i.e., operate in pumping mode in the lower demand seasons. On the other hand, it is assumed that the storage will be fully discharged in the highest demand seasons. i.e., operate in turbine mode to support the grid. Accordingly, $P_{d,t}^p$ and $P_{d,t}^{tur}$ limits should take into consideration the assumed generation capacity and storage capacity. Substituting in equation (3-46), we calculate the required maximum power limits $P_{d,t}^{max}$ for both modes, on the other hand the minimum power limit on $P_{d,t}^{min}$ is considered zero, where $Cycle_D$ is the daily assumed discharging cycle duration in hours and E_s^{max} is the maximum energy storage capacity and $Days_D$ is the number of days the discharging is expected to occur.

$$P_{d,t}^{max} = \frac{E_s^{max}}{Cycle_D \cdot Days_D} \quad (3-46)$$

Table 3-5 summarize the assumptions considered for calculating charging and discharging capacities. The charging shall happen for 270 days, 3 seasons at 6 hours daily and the discharging shall happen for 90 days, 1 season at 6 hours daily.

Table 3-5: Assumptions for charging and discharging capacities

	Charging	Discharging
Daily hours	6	6
Number of seasons	3	1
Days	270	90

3.2.3.4. Penstock

The total length of penstock connecting the lower reservoir to the UR is assumed 490 m. A few fittings are considered in the study, the total $K_{fitting}$ is assumed to be around 10. Penstock diameter can be calculated from equations (3-47) and (3-48). The velocity assumed to be kept 5 m/s. Taking a perfect discharging cycle, the maximum flow should happen in turbine mode when rated power is supplied and when the storage is at its lowest level before it is empty. The maximum flow value will not exceed the flow calculated using (3-49). Substituting with maximum expected flow rate and the assumed velocity, the diameter was found.

$$A = 0.25\pi D^2 \quad (3-47)$$

$$v = \frac{Q_{d,t}^{max}}{A} \quad (3-48)$$

$$Q_{d,t}^{max} = \frac{P_{d,t}^{max}}{n_t \cdot \rho \cdot g \cdot h_z} \quad (3-49)$$

The model assumes one penstock for both pumping and turbine mode, hence the maximum flow to calculate the pipe diameter will be considered from turbine mode since it is higher. Penstock technical parameters are summarized in Table 3-6

Table 3-6: Penstock Technical Parameters

Penstock Material	Carbon Steel	
Absolute roughness ε in mm	0.3 mm	
Relative roughness ε/D	0.00014851	
Diameter	In m	In mm
	2.02	2020
Cross sectional area	3.2 m^2	
Length	490 m	

3.3. Optimization tool

The formulated optimization Problem was built and solved in GAMS, a General Algebraic Modeling System for mathematical optimization and simulations using The Branch-And-Reduce Optimization Navigator solver (BARON). BARON solves nonlinear (NLP) problems globally. The branch-and-bound deterministic global optimization algorithms of the type used in BARON are guaranteed to generate global optima under reasonably generic assumptions; these include the presence of finite lower and upper bounds[53].

Chapter 4. Results and Analysis

In this chapter, we present the simulation results and evaluate the performance of the proposed network. Simulations aim to evaluate the below three aspects of the proposed network:

1. Peak shaving effect; through reflecting the difference in the operation of expensive thermal units before and after PHS unit integration.
2. Charging and discharging decisions as a response to seasonal demand variation.
3. Cost of operation.

4.1. Peak shaving affect

The peak shaving effect was demonstrated by testing the network with and without PHS. However, it is to be noted that during this comparison, the ramp-up and down constraints were removed from the optimization problem, and the minimum limits on thermal units were reduced to zero to be able to observe the contribution of the storage on the reduction of expensive power plants operation without the effect of other constraints. The storage capacity considered in this simulation was 1500MWh.

The OPF was obtained for the network without the PHS unit based on the optimization problem formulated in Chapter 3, except that no ESS was considered, no RU and RD constraints, and the thermal unit lower limits were reduced to zero. Table 4-1 and Figure 4-1 presents the difference of energy production for each unit where negative values indicate a reduction, whereas positive values indicate an increment. Further, Figure 4-2 presents the generation cost for the thermal units per MW to observe the reduction or increment based on unit cost.

Table 4-1:Thermal unit’s energy production before and after PHS unit integration

Thermal Unit	g11	g10	g4	g8	g7	g5	g9	g12	g1	g2	g3	g6
Difference in Energy production MWh/year	288	-558	-387	-396	-153	-18	252	342	396	405	108	0
Total Increase (MWh/year)	1791											
Total Reduction (MWh/year)	-1512											

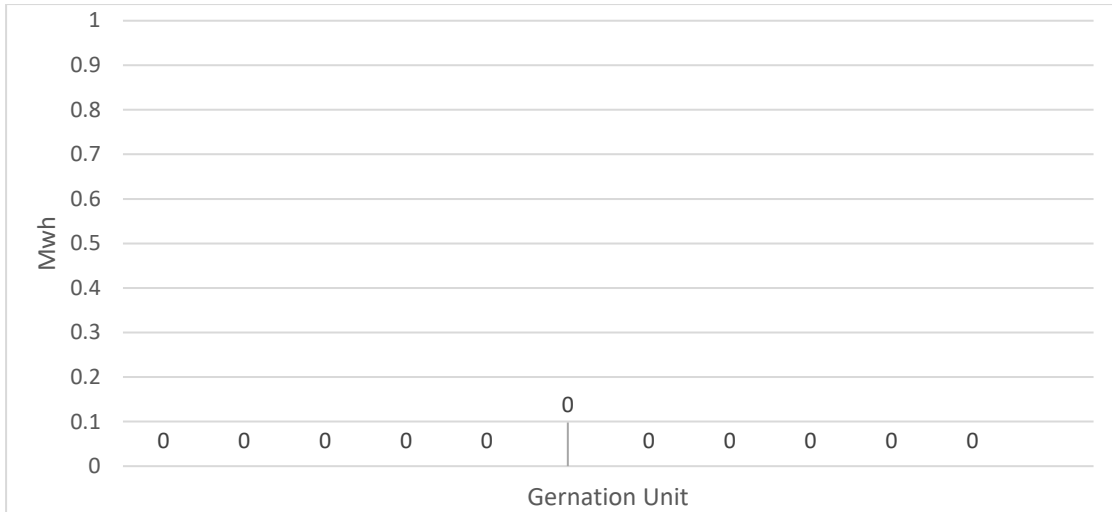


Figure 4-1: Difference in thermal unit's energy production after PHS unit integration

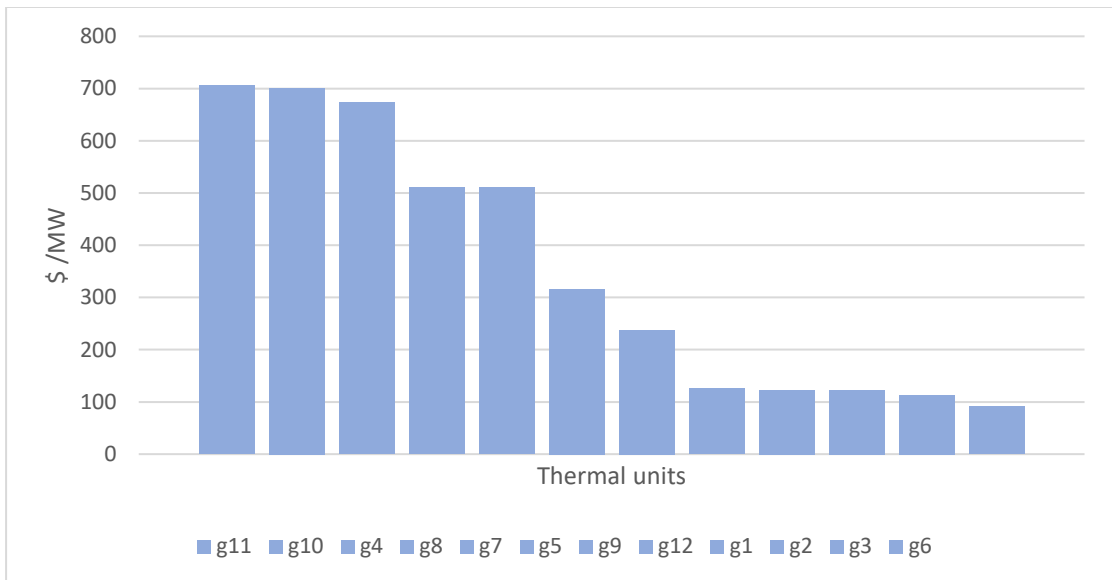


Figure 4-2: Generation cost for the thermal units per MW

4.2. Storage: charging and discharging

To observe the performance of charging and discharging decisions as a response to seasonal demand variations, the average hourly demand for each season in UAE is presented in Figure 4-3, and the water level of the PHS unit UR is plotted against the whole year with a one-hour time interval considering the proposed charging and discharging cycles in Figure 4-4. Further, the proposed PHS was simulated with different charging and discharging (generation) capacities, i.e., lower, and higher than the proposed storage cycle capacities. Figure 4-5 represents the UR level with the increased capacities, in contrast, the plot in Figure 4-6 is for the reduced capacities. The seasons sequence on the UR plots is fall, winter, spring and summer and are

differentiated by colors matching Figure 4-3 of the average hourly seasonal demand. The PHS unit parameters considered in the comparison in this subsection are presented in Table 4-2.

Table 4-2: PHS parameters

Storage Capacity	Storage Parameters		
	h_s	h_z	A
1500MWh	90m	210m	25510m ²

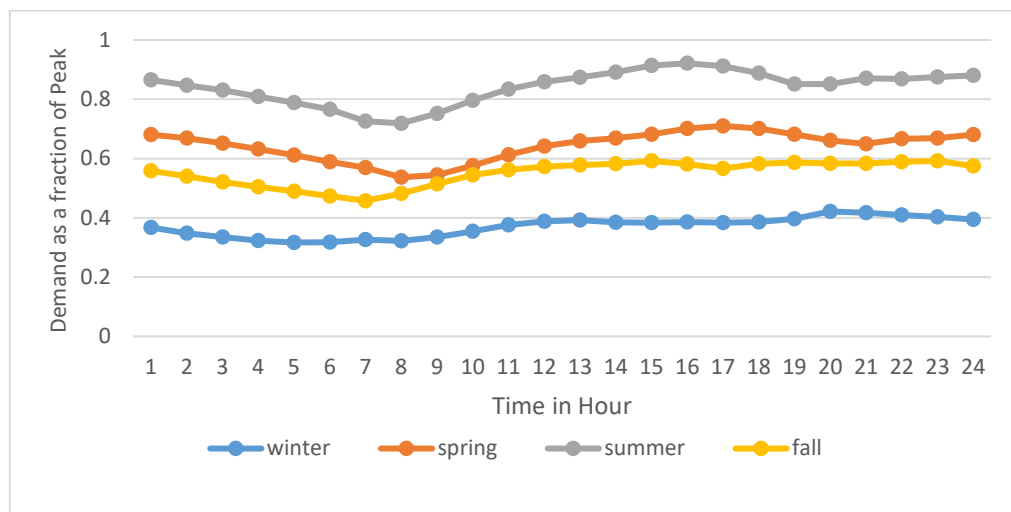


Figure 4-3: Average hourly demand for each season in UAE

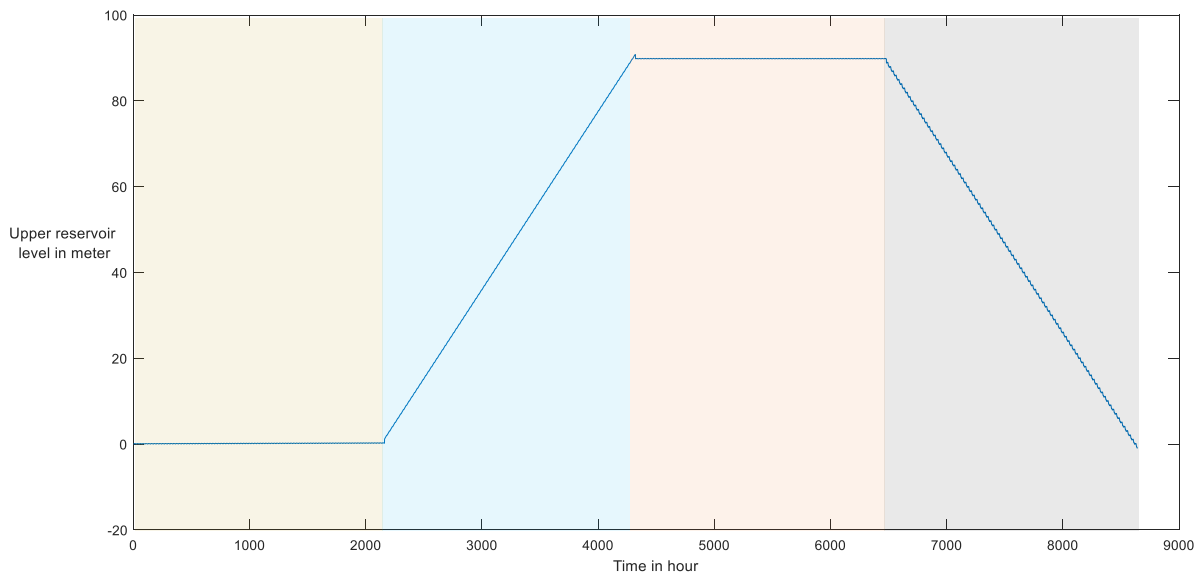


Figure 4-4: Annual level of the UR with proposed charging and discharging capacity

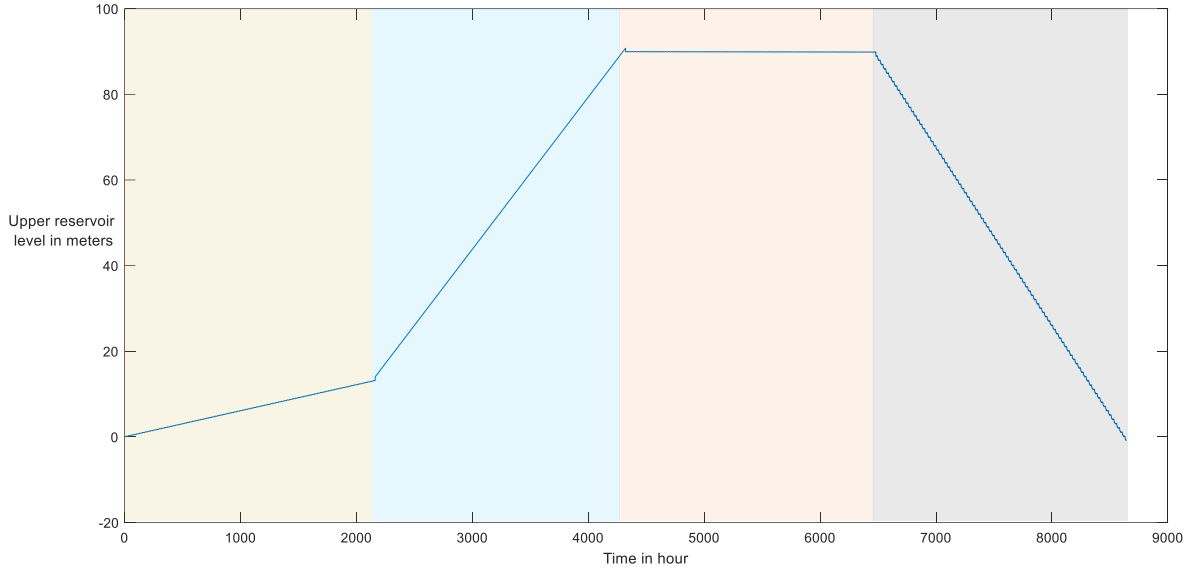


Figure 4-5: Annual level of the UR with decreased charging and discharging capacity

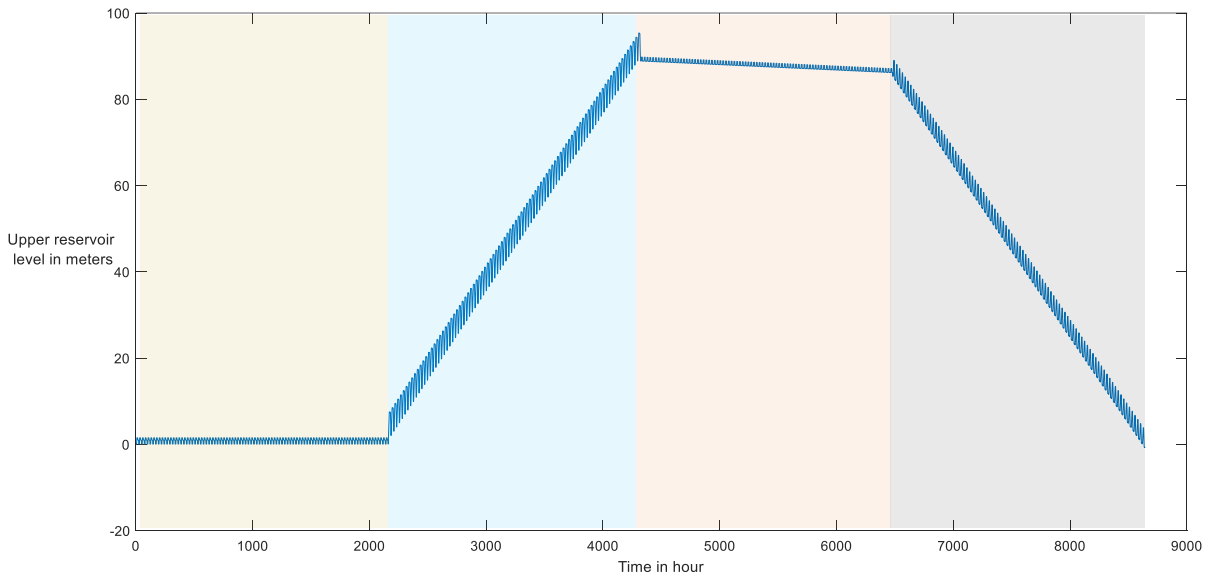


Figure 4-6: Annual level of the UR with increased charging and discharging capacity

4.3. Cost of operation

Generally, the cost of operation encountered reduction due to the peak shaving imposed by the PHS unit. The cost of operation without PHS is 7181 M \$/year; the cost of

operation with PHS and annual reduction are presented in Table 4-3 for different storage capacities. On the other hand,

Table 4-4: Operation cost increasing charging and discharging capacities

PHS Capacity	Operation cost \$	Cost reduction M \$/year
1500MWh	7176	5.5

presents the operation and reduction in cost between the 1500MWh PHS with the increased charging and discharging capacity previously plotted in Figure 4-6 and the 1500 MWh PHS in Figure 4-4, i.e., the one simulated with the proposed charging and discharging cycles.

Table 4-3: Operation cost with different PHS unit storage capacities

PHS Capacity	Operation cost	Cost reduction M \$/year
200MWh	7180	0.98
1500MWh	7179	2.6
15000 MWh	7159	22.56

Table 4-4: Operation cost increasing charging and discharging capacities

PHS Capacity	Operation cost \$	Cost reduction M \$/year
1500MWh	7176	5.5

4.4. Performance evaluation

The results demonstrated that the proposed model successfully simulates the grid-connected PHS's seasonal performance. This was verified by demonstrating the peak shaving effect, the UR level graphs, and the reduction in the operation cost.

The reduction in annual energy production from certain thermal units in the presence of 1500MWh PHS unit reached approximately 1512MWh annually, of which 1224MWh is from the expensive thermal units; hence, it is a good contribution to peak shaving. Further, though unit g6 is the cheapest unit, it didn't produce more energy after integrating the PHS unit because it operates at its maximum limit in both cases. Further, the energy reduction from thermal units is less than the increment due to the system

efficiency; the total increment was 1791 MWh, while the total reduction was 1512MWh. On the other hand, the UR level plots demonstrated that most pumping occurs in the lowest demand season, winter. In contrast, the water level is almost stable in the moderate demand ones, fall, and spring, and then it is fully emptied to support the grid in summer's highest demand season. However, depending on the charging and discharging capacities, the PHS may tend to charge during fall and spring, as shown in Figure 4-5. Further, if charging and discharging capacities are big enough, it may operate to support the grid daily, along with being a seasonal PHS. This is demonstrated in Figure 4-6 and can be easily spotted from the fluctuations observed in the plot. However, this indicates that daily charging and discharging are essential to optimize the cost but knowing the yearly demand trends from the beginning affects the charging and discharging decisions in contrast to if only a day ahead data is predicted or inputted to the optimization problem.

Further, the operation cost obtained for different storage capacities reduced as the storage capacities increased. It is also noticed that increasing the charging and discharging capacities may further reduce the operation cost as the storage charge and discharge daily support the grid.

Chapter 5. Conclusion and Future Work

This research proposed a framework to manage and analyse a grid-connected PHS unit optimally. The proposed framework was deployed to study the seasonal performance of PHS in supporting the grid in the UAE over a study period of one year. The model in this study considers transmission constraints, optimal power flow, and hydraulic model and losses. However, it ignores transmission losses and reactive power. The effectiveness of the proposed framework in simulating the performance of the seasonal PHS unit was demonstrated through several tests to observe the peak shaving effect, the charging and discharging decision as a response to seasonal demand variations, and the operation cost.

It was observed that integrating 1500 MWh PHS reduced the operation of expensive thermal units by 1224MWh annually, and it was evaluated as a good contribution to peak shaving. The UR plots showed that charging mainly occurred in winter, the lowest demand season, whereas discharging was always in the highest demand season, summer. It was concluded that knowing the seasonal trends from an early stage would highly affect the charging and discharging decisions.

Further, a reduction in operation cost was recorded after integrating PHS unit that ranged from 2.6M to 22M \$/year, depending on the storage capacity. Therefore, a trade-off between increasing the construction cost to enlarge the size of PHS and the economic benefits this PHS may contribute should be considered. Further, having an effective seasonal PHS implies that the storage capacity should be sufficient to support the grid in a seasonal basis since a daily PHS plant cannot store energy seasonally. The larger the size of the upper reservoir, the more storage cycles it can perform. The capacity of the PHS unit depends on the water storage capacity of the upper reservoir, the height difference between the upper and lower reservoirs, and the water availability in the lower reservoir.

As a future work, the RTS Network in this model can be replaced with SEWA Network, and improvements to the accuracy of the power flow model by converting it to AC model can be considered. Further, the proposed model could be tested in the presence of a high share of intermittent renewable energy sources (RES). Integrating RES into the network is expected to improve the seasonal storage benefits and overall operational cost and reduce the thermal unit's operation.

References

- [1] M. Uddin, M. F. Romlie, M. F. Abdullah, S. Abd Halim, A. H. Abu Bakar, and T. Chia Kwang, "A review on peak load shaving strategies," *Renewable and Sustainable Energy Reviews*, vol. 82, pp. 3323–3332, Feb. 2018, doi: 10.1016/J.RSER.2017.10.056.
- [2] "Peak shaving - Off grid system - AE Solar." Accessed Dec. 11, 2022 [Online]. Available: <https://ae-solar.com/peak-shaving-off-grid-system/>.
- [3] J. Cochran *et al.*, "Flexibility in 21st Century Power Systems", Accessed: Nov. 17, 2022. [Online]. Available: <https://www.nrel.gov/docs/fy14osti/61721.pdf>
- [4] A. E. Samani, A. D'Amicis, J. D. M. de Kooning, D. Bozalakov, P. Silva, and L. Vandeveld, "Grid balancing with a large-scale electrolyser providing primary reserve," *IET Renewable Power Generation*, vol. 14, no. 16, pp. 3070–3078, Dec. 2020, doi: 10.1049/IET-RPG.2020.0453.
- [5] F. Nadeem, S. M. Suhail Hussain, P. K. Tiwari, A. K. Goswami, and T. Selim Ustun, "Comparative Review of Energy Storage Systems, Their Roles, and Impacts on Future Power Systems", doi: 10.1109/ACCESS.2018.2888497.
- [6] T. M. Masaud, K. Lee and P. K. Sen, "An overview of energy storage technologies in electric power systems: What is the future?," *North American Power Symposium 2010*, Arlington, TX, USA, 2010, pp. 1-6, doi: 10.1109/NAPS.2010.5619595.
- [7] P. Medina, A. W. Bizuayehu, J. P. S. Catalão, E. M. G. Rodrigues, and J. Contreras, "Electrical energy storage systems: Technologies' state-of-the-art, techno-economic benefits and applications analysis," *Proceedings of the Annual Hawaii International Conference on System Sciences*, pp. 2295–2304, 2014, doi: 10.1109/HICSS.2014.290.
- [8] L. Stoyanov, A. Sadovski, G. Notton, V. Lazarov, and L. Stoyanov, "Analysis of Pumped Hydroelectric Storage for a Wind/PV System for Grid Integration."

- [9] “Hydraulic head - Energy Education.” Accessed Sep. 30, 2022 [Online] Available: https://energyeducation.ca/encyclopedia/Hydraulic_head#cite_note-RE1-2.
- [10] G. T. Bitew, M. Han, S. A. Mekonnen, S. Patrobers, Z. W. Khan, and L. K. Tuan, “Pumped energy storage system technology and its AC–DC interface topology, modelling and control analysis: a review,” *The Journal of Engineering*, vol. 2019, no. 16, pp. 705–710, Mar. 2019, doi: 10.1049/JOE.2018.8379.
- [11] F. Díaz-González, A. Sumper, O. Gomis-Bellmunt, and R. Villafáfila-Robles, “A review of energy storage technologies for wind power applications,” *undefined*, vol. 16, no. 4, pp. 2154–2171, May 2012, doi: 10.1016/J.RSER.2012.01.029.
- [12] J. C. Beardsall, C. A. Gould and M. Al-Tai, "Energy storage systems: A review of the technology and its application in power systems," 2015 50th International Universities Power Engineering Conference (UPEC), Stoke on Trent, UK, 2015, pp. 1-6, doi: 10.1109/UPEC.2015.7339794.
- [14] “Surface Reservoir Pumped Hydroelectric Storage | ESA.” Accessed Sep. 22, 2022 [Online]. Available: <https://energystorage.org/why-energy-storage/technologies/surface-reservoir-pumped-hydroelectric-storage/>.
- [15] J. D. Hunt, B. Zakeri, A. Nascimento, and R. Brandão, “Pumped hydro storage (PHS),” *Storing Energy: with Special Reference to Renewable Energy Sources*, pp. 37–65, Jan. 2022, doi: 10.1016/B978-0-12-824510-1.00008-8.
- [16] S. Rehman, L. M. Al-Hadhrami, and M. M. Alam, “Pumped hydro energy storage system: A technological review,” *Renewable and Sustainable Energy Reviews*, vol. 44, pp. 586–598, Apr. 2015, doi: 10.1016/J.RSER.2014.12.040.
- [17] R. L. Murray and K. E. Holbert, “Energy,” *Nuclear Energy*, pp. 3–13, Jan. 2020, doi: 10.1016/B978-0-12-812881-7.00001-0.
- [18] I. Tosun, “STEADY MICROSCOPIC BALANCES WITH GENERATION,” *Modeling in Transport Phenomena*, pp. 305–407, Jan. 2007, doi: 10.1016/B978-044453021-9/50010-5.

- [19] S. Ge, “HYDROLOGY | Ground and Surface Water,” *Encyclopedia of Atmospheric Sciences*, pp. 973–979, Jan. 2003, doi: 10.1016/B0-12-227090-8/00171-8.
- [20] R. Gentle, P. Edwards, and B. Bolton, “Fluid mechanics,” *Mechanical Engineering Systems*, pp. 112–168, Jan. 2001, doi: 10.1016/B978-075065213-1/50003-9.
- [21] P. Bajpai, “Hydraulics,” *Biermann’s Handbook of Pulp and Paper*, pp. 455–482, Jan. 2018, doi: 10.1016/B978-0-12-814238-7.00023-4.
- [22] M. McWilliams, “Pumped Storage Hydropower,” in *Comprehensive Renewable Energy*, Elsevier, 2022, pp. 147–175. doi: 10.1016/b978-0-12-819727-1.00079-0.
- [23] R. J. Kerkman, T. A. Lipo, and W. G. Newman, “An Inquiry into Adjustable Speed Operation of a Pumped Hydro Plant Part 1 - Machine Design and Performance,” 1980. doi: 10.1109/TPAS.1980.319773.
- [24] E. Muljadi, R. M. Nelms, E. Chartan, R. Robichaud, L. George, and H. Obermeyer, “Electrical Systems of Pumped Storage Hydropower Plants: Electrical Generation, Machines, Power Electronics, and Power Systems,” 2021, Accessed: Sep. 25, 2022. [Online]. Available: <https://www.nrel.gov/docs/fy21osti/74721.pdf>.
- [25] “Practical Power System Operation | IEEE eBooks | IEEE Xplore.” Accessed Dec. 21, 2022 [Online]. Available: <https://ieeexplore.ieee.org/book/6774611>
- [26] A. Soroudi, *Power system optimization modeling in GAMS*. Springer International Publishing, 2017. doi: 10.1007/978-3-319-62350-4.
- [27] D. van Hertern, J. Verboornen, K. Purchala, R. Belrnans, and W. L. KlingH, “Usefulness of DC Power Flow for Active Power Flow Analysis with Flow Controlling Devices.”
- [28] D. W. Ross and S. Kim, “Dynamic economic dispatch of generation,” *IEEE Transactions on Power Apparatus and Systems*, vol. PAS-99, no. 6, pp. 2060–2068, 1980, doi: 10.1109/TPAS.1980.319847.

- [29] E. Zondervan and I. E. Grossmann, “Multi-objective optimization of energy networks under demand uncertainty,” *Computer Aided Chemical Engineering*, vol. 38, pp. 2319–2324, 2016, doi: 10.1016/B978-0-444-63428-3.50391-X.
- [30] J. K. Pattanaik, M. Basu, and D. P. Dash, “Dynamic economic dispatch: a comparative study for differential evolution, particle swarm optimization, evolutionary programming, genetic algorithm, and simulated annealing,” *Journal of Electrical Systems and Information Technology 2019 6:1*, vol. 6, no. 1, pp. 1–18, Nov. 2019, doi: 10.1186/S43067-019-0001-4.
- [31] X. Liu, M. Ding, J. Han, P. Han, and Y. Peng, “Dynamic economic dispatch for microgrids including battery energy storage,” *2nd International Symposium on Power Electronics for Distributed Generation Systems, PEDG 2010*, pp. 914–917, 2010, doi: 10.1109/PEDG.2010.5545768.
- [32] A. Nawaz, E. Mustafa, N. Saleem, M. I. Khattak, M. Shafi, and A. Malik, “Solving convex and non-convex static and dynamic economic dispatch problems using hybrid particle multi-swarm optimization,” *Tehnicki Vjesnik*, vol. 24, no. 4, pp. 1095–1102, 2017, doi: 10.17559/TV-20150720093711.
- [33] O. D. Montoya Giraldo, “Solving a Classical Optimization Problem Using GAMS Optimizer Package: Economic Dispatch Problem Implementation,” *Ing Cienc*, vol. 13, no. 26, pp. 39–63, Nov. 2017, doi: 10.17230/INGCIENCIA.13.26.2.
- [34] I. Ahmed, U.-E.-H. Alvi, A. Basit, T. Khursheed, A. Alvi, K.-S. Hong, and M. Rehan, “A novel hybrid soft computing optimization framework for dynamic economic dispatch problem of complex non-convex contiguous constrained machines,” *PLOS ONE*, vol. 17, no. 1, 2022.
- [35] D. W. Ross and S. Kim, “Dynamic Economic Dispatch of Generation,” 1980, doi: 10.1109/TPAS.1980.319847.
- [36] M. Tuffaha and J. T. Gravdahl, “Dynamic formulation of the unit commitment and economic dispatch problems,” *Proceedings of the IEEE International Conference on Industrial Technology*, vol. 2015-June, no. June, pp. 1294–1298, Jun. 2015, doi: 10.1109/ICIT.2015.7125276.

- [37] J. Lin, F. Magnago, and J. M. Alemany, “Optimization methods applied to power systems: Current practices and challenges,” in *Classical and Recent Aspects of Power System Optimization*, Elsevier Inc., 2018, pp. 1–18. doi: 10.1016/B978-0-12-812441-3.00001-X.
- [38] K. Kusakana, “Optimal scheduling for distributed hybrid system with pumped hydro storage,” *Energy Convers Manag*, vol. 111, pp. 253–260, Mar. 2016, doi: 10.1016/j.enconman.2015.12.081.
- [39] M. Basu, “Fuel constrained dynamic economic dispatch with demand side management,” *Energy*, vol. 223, May 2021, doi: 10.1016/j.energy.2021.120068.
- [40] B. Zhou, S. Liu, S. Lu, X. Cao, and W. Zhao, “Cost–benefit analysis of pumped hydro storage using improved probabilistic production simulation method,” *The Journal of Engineering*, vol. 2017, no. 13, pp. 2146–2151, Jan. 2017, doi: 10.1049/joe.2017.0709.
- [41] P. T. Mary, C. H. Ram Jethmalani, and S. P. Simon, “Thermal unit commitment considering pumped storage hydro electricity plants,” in *2013 International Conference on Energy Efficient Technologies for Sustainability, ICEETS 2013*, 2013, pp. 964–969. doi: 10.1109/ICEETS.2013.6533517.
- [42] A. Ghasemi and M. Enayatzare, “Optimal energy management of a renewable-based isolated microgrid with pumped-storage unit and demand response,” *Renew Energy*, vol. 123, pp. 460–474, Aug. 2018, doi: 10.1016/j.renene.2018.02.072.
- [43] S. Makhdoomi and A. Askarzadeh, “Optimizing operation of a photovoltaic/diesel generator hybrid energy system with pumped hydro storage by a modified crow search algorithm,” *J Energy Storage*, vol. 27, Feb. 2020, doi: 10.1016/j.est.2019.101040.
- [44] J. Yang, S. Zhang, J. Liu, X. Han, W. Peng, and J. Liu, “Dynamic Dispatch Of Hybrid Hydro/PV/PHS Complementary Power Generation System Based On Deep Reinforcement Learning,” in *5th IEEE Conference on Energy Internet and Energy System Integration: Energy Internet for Carbon Neutrality, EI2 2021*, 2021, pp. 2125–2129. doi: 10.1109/EI252483.2021.9713216.

- [45] M. Basu, “Combined heat and power dynamic economic dispatch with demand side management incorporating renewable energy sources and pumped hydro energy storage,” *IET Generation, Transmission and Distribution*, vol. 13, no. 17, pp. 3771–3781, Sep. 2019, doi: 10.1049/iet-gtd.2019.0216.
- [46] B. S. Pali and S. Vadhera, “A novel pumped hydro-energy storage scheme with wind energy for power generation at constant voltage in rural areas,” *Renew Energy*, vol. 127, pp. 802–810, Nov. 2018, doi: 10.1016/j.renene.2018.05.028.
- [47] Z. Liu, Z. Zhang, R. Zhuo, and X. Wang, “Optimal operation of independent regional power grid with multiple wind-solar-hydro-battery power,” *Appl Energy*, vol. 235, pp. 1541–1550, Feb. 2019, doi: 10.1016/j.apenergy.2018.11.072.
- [48] L. Wen, K. Suomalainen, B. Sharp, M. Yi, and M. S. Sheng, “Impact of wind-hydro dynamics on electricity price: A seasonal spatial econometric analysis,” *Energy*, vol. 238, Jan. 2022, doi: 10.1016/j.energy.2021.122076.
- [49] S. Daneshgar and R. Zahedi, “Investigating the hydropower plants production and profitability using system dynamics approach,” *J Energy Storage*, vol. 46, Feb. 2022, doi: 10.1016/j.est.2021.103919.
- [50] D. Paluszczyszyn, “Advanced modelling and simulation of water distribution systems with discontinuous control elements,” *De Montfort University* 2015.
- [51] N. Mousavi, G. Kothapalli, D. Habibi, M. Khiadani, and C.K. Das, “An improved mathematical model for a pumped hydro storage system considering electrical, mechanical, and hydraulic losses,” *Appl Energy*, vol. 247, pp. 228–236, Aug. 2019, doi: 10.1016/j.apenergy.2019.03.015.
- [52] M. Simão and H. M. Ramos, “Hybrid Pumped Hydro Storage Energy Solutions towards Wind and PV Integration: Improvement on Flexibility, Reliability and Energy Costs,” *Water 2020, Vol. 12, Page 2457*, vol. 12, no. 9, p. 2457, Sep. 2020, doi: 10.3390/W12092457.
- [53] N. Sahinidis “BARON.” Accessed Nov. 17, 2022 [Online]. Available: https://www.gams.com/latest/docs/S_BARON.html

Appendix A

hour	Demand	hour	demand	hour	demand
1	1046.679	40	1997.383	79	1304.027
2	991.188	41	2023.827	80	1372.961
3	955.358	42	1997.197	81	1464.509
4	922.389	43	1943.83	82	1551.197
5	902.836	44	1885.735	83	1599.959
6	904.662	45	1851.734	84	1631.465
7	931.494	46	1899.695	85	1646.707
8	916.87	47	1905.074	86	1660.284
9	954.083	48	1938.836	87	1687.089
10	1011.225	49	2464.722	88	1655.241
11	1071.214	50	2414.778	89	1614.463
12	1105.701	51	2366.593	90	1658.364
13	1117.089	52	2306.389	91	1671.444
14	1096.529	53	2248.884	92	1663.561
15	1091.936	54	2182.932	93	1662.889
16	1099.255	55	2068.459	94	1676.829
17	1094.783	56	2048.396	95	1686.109
18	1099.51	57	2142.899	96	1637.682
19	1129.646	58	2267.605		
20	1201.52	59	2377.511		
21	1188.064	60	2447.788		
22	1166.98	61	2491.071		
23	1149.508	62	2539.403		
24	1122.971	63	2605.02		
25	1939.939	64	2625.5		
26	1906.455	65	2597.164		
27	1856.183	66	2531.077		
28	1801.103	67	2425.629		
29	1741.401	68	2425.831		
30	1676.944	69	2481.966		
31	1621.851	70	2476.513		
32	1529.303	71	2494.079		
33	1552.383	72	2508.986		
34	1640.924	73	1592.264		
35	1745.505	74	1539.567		
36	1829.991	75	1485.164		
37	1879.387	76	1436.899		
38	1905.379	77	1393.588		
39	1943.843	78	1347.995		

Vita

Asmaa Ibrahim was born in 1994, in Dubai, United Arab Emirates. She received her primary and secondary education in Dubai, UAE. She received her B.Sc. degree in Electrical and Electronic Engineering from University of Sharjah in 2017.

In September 2017, she joined the Electrical Engineering master's program in the American University of Sharjah as a part time student and during her master's study, she started her career as a full-time electrical engineer. Her research interests are in Energy storage systems.